

of immune responses and by presenting pathogen specific antigen to T cells, followed by enhancement of appropriate defensive immunity. Conversely, B cells work as “rascals” in the exacerbation stage of autoimmunity through presenting autoantigens to autoreactive T cells, resulting in autoimmunity going out of control. Recognition of this paradigm for the role of B cells in regulating the magnitude of immune response will help to facilitate both basic and clinical research on the regulation of immune responses.

## REFERENCES

1. Dörner T, Radbruch A, Burmester G.R. (2009) B-cell-directed therapies for autoimmune disease. *Nat Rev Rheumatol* **5**: 433–41.
2. Levesque M.C. (2009) Translational mini-review series on B cell-directed therapies: recent advances in B cell-directed biological therapies for autoimmune disorders. *Clin Exp Immunol* **157**: 198–208.
3. Mease P.J. (2008) B cell-targeted therapy in autoimmune disease: rationale, mechanisms, and clinical application. *J Rheumatol* **35**: 1245–55.
4. Pescovitz M.D., Greenbaum C.J., Krause-Steinrauf H., Becker D.J., Gitelman S.E., Golland R., et al. (2009) Rituximab, B-lymphocyte depletion, and preservation of beta-cell function. *N Engl J Med* **361**: 2143–52.
5. Suarez-Pinzon W.L., Rabinovitch A. (2001) Approaches to type 1 diabetes prevention by intervention on cytokine immunoregulatory circuits. *Int J Exp Diab Res* **2**: 3–17.
6. Silverman G.J., Boyle D.L. (2008) Understanding the mechanistic basis in rheumatoid arthritis for clinical response to anti-CD20 therapy: the B-cell roadblock hypothesis. *Immunol Rev* **223**: 175–85.
7. Sanz I. (2009) The conundrum of B cell depletion in SLE. *Nat Rev Rheumatol* **5**: 304–5.
8. Schlomchik M.J. (2009) Activating systemic autoimmunity: B's, T's, and tolls. *Curr Opin Immunol* **21**: 626–33.
9. Lund F.E. (2008) Cytokine-producing B-lymphocytes-key regulators of immunity. *Curr Opin Immunol* **20**: 332–338.
10. Armed R., Carvone F., Ley T., O'Garra A., Reiner S., Schreiber R., et al. (2008) Dendritic cells process antigen from a wide array of pathogens. In: Murphy K., Traversm P., Walport M., eds. *Janeway's Immunobiology*, 7th edn. New York and London: Garland Science, pp. 334–6.
11. Jaiswal A.I., Croft M. (1997) CD40 ligand induction of T cell subsets by peptide-presenting B cells. *J Immunol* **159**: 2282–91.
12. Nagafuchi S., Katsuta H., Anzai K. (2010) Rituximab, B-lymphocyte depletion, and beta-cell function. *N Engl J Med* **362**: 761.
13. Kondo S., Iwata I., Anzai K., Akashi T., Wakana S., Ohkubo K., et al. (2000) Suppression of insulinitis and diabetes in B cell-deficient mice treated with streptozocin: B cells are essential for T cell receptor clonotype spreading in islet-infiltrating T cells. *Int Immunol* **12**: 1075–83.
14. Akashi T., Nagafuchi S., Kitamura D., Anzai K., Wang J., Taniuchi I., et al. (1977) Direct evidence for the contribution of B cells to the progression of insulinitis and the development of diabetes in non-obese diabetic mice. *Int Immunol* **9**: 1159–1164.
15. Hu Cy., Rodriguez-Pinto D., Du W., Ahuja A., Henegarju O., Wong F.S., et al. (2007) Treatment with CD20-specific antibody prevents and reverses autoimmune diabetes in mice. *J Clin Invest* **117**: 3857–67.
16. Xiu Y., Wong C.P., Bounaziz J.D., Hamaguchi Y., Wang Y., Pop S.M., et al. (2008) B lymphocyte depletion by CD20 monoclonal antibody prevents diabetes in non-obese diabetic mice despite isotype-specific differences in FcγR effector functions. *J Immunol* **180**: 2863–75.
17. Barnadas M.A., Roe E., Brunet S., Garcia P., Bergua P., Pimentel L., et al. (2006) Therapy of paraneoplastic pemphigus with Rituximab: a case report and review of literature. *JEADV* **20**: 69–74.
18. Lutt J.R., Pisculli M.L., Weinblatt M.E., Deodhar A., Winthrop K.L. (2008) Severe nontuberculous mycobacterial infection in 2 patients receiving Rituximab for refractory myositis. *J Rheumatol* **35**: 1683–86.
19. Laubach J., Bawn S.D., Gordon L.I., Winter J.N., Furman R.R., Vose J.M., et al. (2009) Progressive multifocal leukoencephalopathy after rituximab therapy in HIV-negative patients: a report of 57 cases from the Research on Adverse Drug Events and Reports project. *Blood* **113**: 4834–40.
20. Bayry J., Lacroix-Desmazes S., Kazatchkine M.D., Kaveri S.V. (2004) Intravenous immunoglobulin for infectious diseases: back to the pre-antibiotic and passive prophylaxis era?. *Trends Pharmacol Sci* **25**: 305–10.

# ウイルス糖尿病と 自己免疫性1型糖尿病

NAGAFUCHI SEIHO

永淵正法

◎九州大学医学研究院保健学部門検査技術科学分野病態情報学

**要旨** 多くの臨床的あるいは基礎的研究からウイルスが糖尿病発症の原因であることが強く示唆されているが、決定的な証拠は乏しい。ウイルス感染症による糖尿病発症機構の解明には、ウイルスと宿主要因のいずれをも明らかにすることが必要である。

## はじめに

ウイルス感染症が糖尿病の発症要因の一つとして注目されつつある<sup>1,2)</sup>。歴史的にも、糖尿病発症の原因として、重症のウイルス感染症に伴う全身臓器障害の膵病変として膵島にウイルスが存在することが、しばしば報告されている<sup>3)</sup>。さらに、最近、急性ウイルス感染を伴い発症した1型糖尿病、特に膵炎を伴う劇症1型糖尿病でウイルスが原因であるとする傍証が蓄積されている<sup>4)</sup>。また、実験研究では、脳心筋炎(EMC)ウイルスを用いて、糖尿病誘発性の高い変異株(EMC-D)ウイルスの特性、感染防御、膵島細胞障害のメカニズムなど、基礎的研究の知見が蓄積されている<sup>5,6)</sup>。このように多くの臨床的あるいは基礎的研究からウイルスが糖尿病発症の原因であることが強く示唆されるが、臨床的に分離されたウイルスが実験動物に糖尿病を誘発したことを証明した報告はまれである(表1)。今回は糖尿病の発症原因としてのウイルス感染を、感染防御システム障害や自己免疫誘導のトリガーとして考えながら議論したい。

## ■糖尿病の病因としてのウイルスの位置づけ

ウイルスによる糖尿病は、日本糖尿病学会の分類では二次性糖尿病の「他の疾患、条件に伴うもの」の「(5)感染症」に分類されている(表2)。すなわち、風疹ウイルス(先天性風疹)、サイトメガロウイルス、ヒトヘルペスウイルス6、コクサッキーウイルス、ムンプスウイルスなどが糖尿病の原因になりうると認識されている(表1)。なかでも、先天性風疹児に併発する糖尿病は、ウイルス原因説の有力な根拠である。一方、1型糖尿病では、自己免疫で発症するタイプAと、特発性と称するタイプB分類に分類されているが、タイプBの原因の主な候補としてウイルスがあげられる。1型糖尿病の約20%、そのサブタイプである急激な発症様式を示す劇症1型糖尿病患者では約70%の症例に発熱、上気道炎など風邪症状を伴うことから、いわゆる風邪ウイルスが1型糖尿病発症の原因であることが疑われている(表1)。

表1 糖尿病ウイルス原因説と候補ウイルス

糖尿病ウイルス原因説の根拠	候補ウイルス
1. 重症の全身ウイルス感染症では血糖が上昇し、膵島にウイルスが存在することが繰り返し報告されてきた。	ヒト    コクサッキーウイルス (エンテロウイルス) A型肝炎ウイルス
2. 1型糖尿病の約20%、そのサブタイプである急激な発症様式を示す劇症1型糖尿病患者では約70%の症例に、発熱、上気道炎など風邪症状を伴い、膵島にウイルスが存在することが報告されている。	風疹ウイルス ムンプスウイルス ロタウイルス サイトメガロウイルス
3. 実験的に、特殊なウイルス株を用いて、糖尿病を誘発できる。	ヒトヘルペスウイルス6
*ただし、ヒトから分離されたウイルスが実験動物で糖尿病を発症することを証明した報告は乏しい(コホの三原則が満たされていない)。	動物    コクサッキーウイルス 脳心筋炎ウイルス レオウイルス

文献1)より

表2 糖尿病の成因分類

I. 1型    膵島β細胞の破壊、通常は絶対的インスリン不足に至る
A. 自己免疫性
B. 特発性
II. 2型    インスリン分泌低下を主体とするものと、インスリン抵抗性が主体で、それにインスリンの相対的不足を伴うものなどがある
III. その他の特定の機序、疾患によるもの
A. 遺伝因子として遺伝子異常が同定されたもの
B. 他の疾患、条件に伴うもの
IV. 妊娠糖尿病

## ■ウイルスに対する感染防御システム

ウイルス感染の抵抗性にかかわる第一線の防御は物理的、化学的障壁である皮膚粘膜である。皮膚粘膜は洗浄作用のある物理的なバリアであるのみでなく、汗や粘液中には、それぞれ乳酸や脂肪酸、ムチン、リゾチーム、ラクトフェリン、ディフェンシンなどが含まれ、洗浄作用のみならず抗ウイルス作用を発揮する。

次に、自然免疫と称される、貪食、インターフェロンなどによるウイルス増殖抑制があげられる。ウイルスは、病原体関連分子パターン(pathogen

associated molecular pattern: PAMP) を認識する PRR (pattern recognition receptor) によって捕捉され、その刺激によって誘導される interferon releasing factor によって活発に遺伝子が発現し、インターフェロンが産生され、細胞外に放出される。遊離したインターフェロンは、インターフェロンレセプターに結合し、その刺激により JAK-Stat 経路を介して RNase などの抗ウイルス因子が産生されることによって抗ウイルス活性が発揮される<sup>7)</sup>。さらに、PRR を発現している樹状細胞がウイルス抗原を処理して T 細胞に提示することにより、ウイルス感染防御の主体を担う Th1 タイプの免疫応答が惹起される。Th1 反応は IL-12 によって誘導される転写因子 T-bet の作用により T 細胞から IL-2, interferon  $\gamma$  (IFN  $\gamma$ ), tumor necrosis factor- $\beta$  (TNF- $\beta$ ) が分泌され、活性化マクロファージや細胞傷害性 T 細胞などの細胞性免疫と、主要な IgG 抗体を誘導することによりウイルス感染を制御する<sup>8)</sup>。一方、C 型肝炎のインターフェロン治療中に膵島細胞に自己免疫が誘導される(膵島細胞自己抗体) ことにより 1 型糖尿病が発症することもよく知られていて、免疫応答の二面性、すなわち生体を守ることも、むしろ障害に傾くこともありうる事が理解できる<sup>9)</sup>。

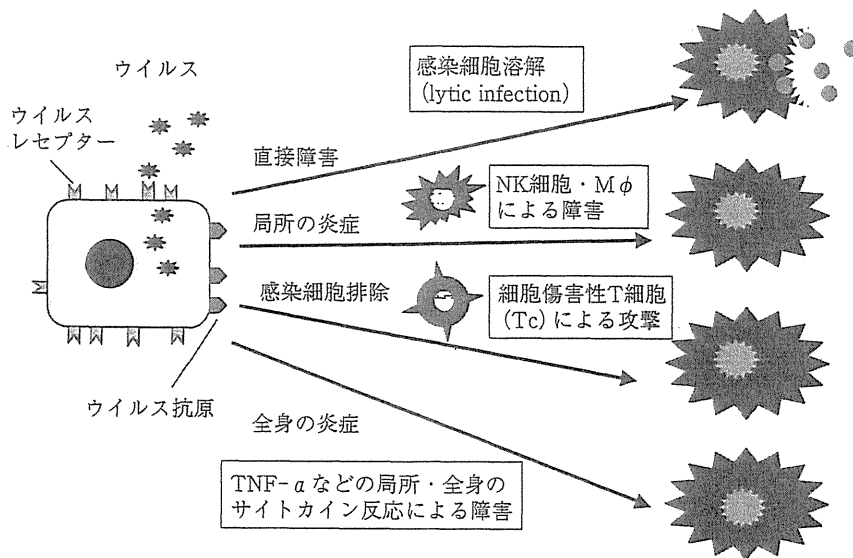


図 1a ウイルス感染によって惹起される膵島細胞障害のメカニズム

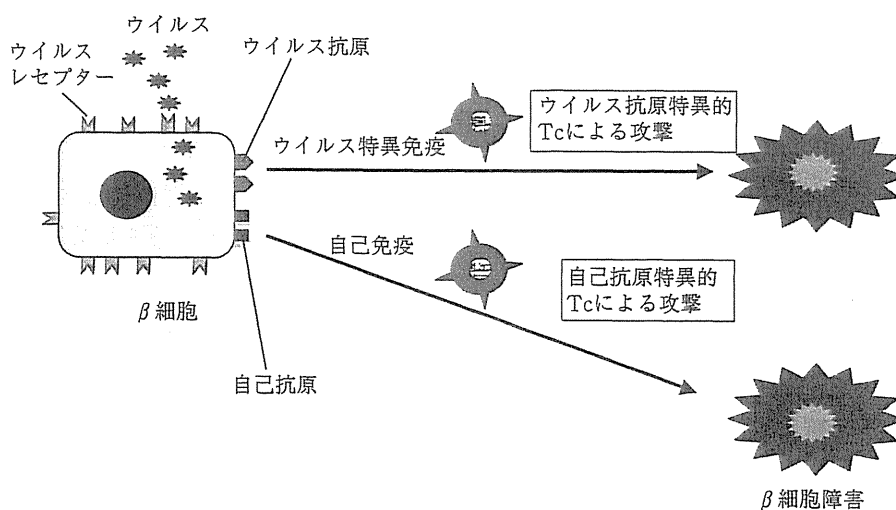


図 1b ウイルス感染細胞に対するウイルス特異的あるいは自己抗原特異的細胞傷害性 T 細胞の誘導

## ■ウイルスによる膵島細胞障害と糖尿病発症

ウイルス感染症が糖尿病を誘発する過程には、多くのメカニズムが想定される。具体的には、①ウイルスによる直接障害、②ウイルス感染細胞に対する特異的あるいは非特異的免疫機序による障害、③惹起された炎症細胞が放出する細胞傷害性物質による障害、などが考えられる (図 1a)。さらに、④ウイルス感染を契機として膵島β細胞特異的自己免疫が誘導されることもありうる<sup>10)</sup>。

## ■ウイルス感染をトリガーとした特異的自己免疫応答の活性化とその制御

### 1. ウイルス感染防御と自己免疫応答

ウイルス感染細胞は、偏性細胞内寄生体であるため、その増殖に宿主の複製機能を必要とする。その過程で、初期の核酸合成酵素などの早期抗原 (early antigen) は細胞表面に表出され、通常ウイルス特異的であるため、ウイルス抗原特異的細胞傷害性 T 細胞の標的となり、ウイルス感染細胞を障害排除する。その結果、成熟ウイルス粒子

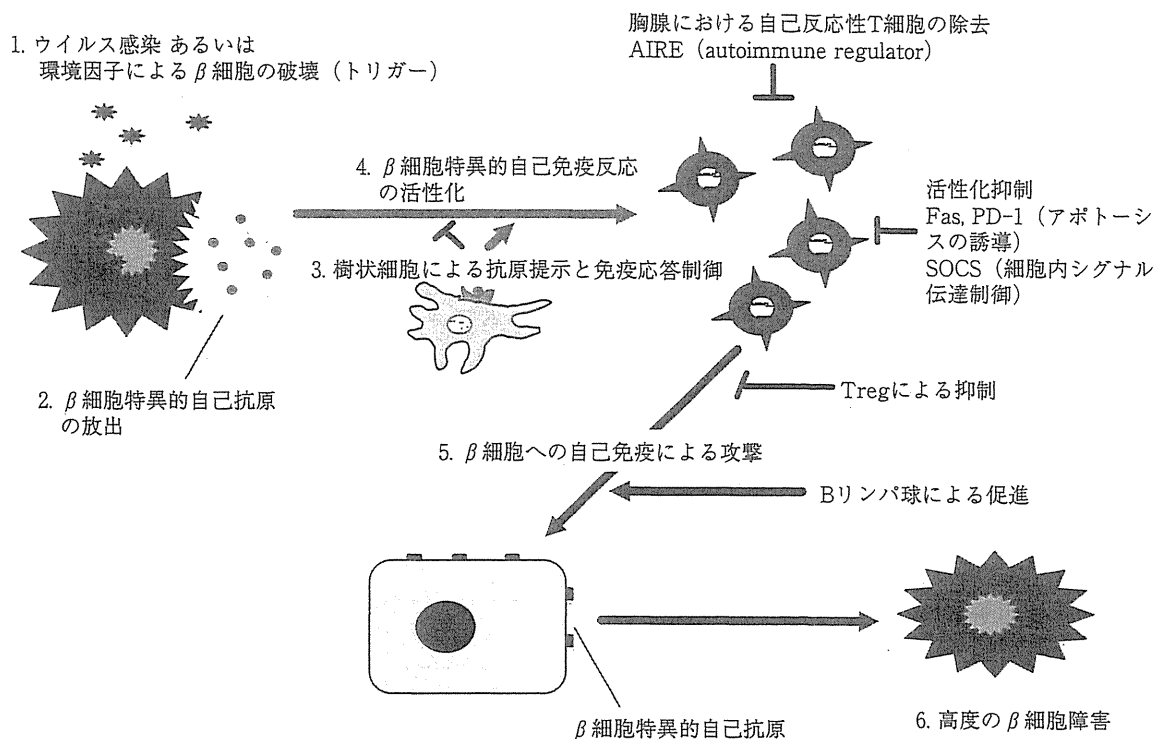


図2 ウイルス感染をトリガーとした膵島β細胞に対する自己免疫の誘導とその制御機構

の完成前に細胞機能が障害され、ウイルス増殖が抑制される。このことは、ウイルス抗原に対する免疫応答であるが、結果として自己細胞の障害に働くため、一面、自己免疫応答と類似する臨床像を呈しうる（図1b）。例えば、持続的感染をきたす代表疾患である肝炎ウイルスによるウイルス性肝炎、あるいは自己免疫性肝炎も肝細胞を障害することは同一の臨床像を呈し、その鑑別は困難である。膵島感染細胞に対する免疫応答にも同様のことが生じる可能性がある。慢性ウイルス感染としては、サイトメガロウイルス再活性化と免疫的膵島細胞障害は、そのよいモデルであると考えられる<sup>11)</sup>。

## 2. 自己抗原の遊離とその認識

前述したようにウイルス感染細胞の障害により隠蔽されている自己抗原の表出誘導や自己抗原の遊離は、その後の自己反応性の惹起に働くことは容易に考えられる。そもそも自己反応性T細胞、あるいはβ細胞は、生体に少数であるが存在して

いることはよく知られているので、ウイルス感染細胞障害による自己抗原の提示により、このような非活性化状態の自己免疫反応がより強く、かつ継続して活性化されることは十分にありうる。ただし、その場合、自己免疫応答制御機構の障害、あるいは破綻が伴って初めて自己免疫糖尿病の発症につながるのであろう。

## 3. 自己免疫応答制御機構の破綻と1型糖尿病

自己反応性は、様々なメカニズムで制御されている。最近の免疫学のトピックとして、中枢性の自己反応性T細胞の除去に働く自己免疫調節遺伝子AIREの同定と、末梢における自己反応性を制御するFoxp3<sup>+</sup>CD25<sup>+</sup>CD4<sup>+</sup>調節性T細胞(Treg)の発見は、この分野に目覚ましい進歩をもたらした<sup>12,13)</sup>。AIRE遺伝子変異によりカンジダ症と臓器特異的の自己免疫が生じる。自己免疫の標的臓器は、一般に、副腎、副甲状腺が中心であるが、HLAタイプが1型糖尿病感受性であれば、1型糖尿病を合併し、1型糖尿病抵抗性では、む

しる典型的なアジソン病と副甲状腺機能低下の臨床像を呈する<sup>14)</sup>。一方, Treg の欠損では, むしろ 1 型糖尿病は主徴の一つである<sup>13)</sup>。このことは, Treg による末梢性の免疫応答調節が自己免疫糖尿病発症制御に, より重要であることを示唆している。

上述のウイルス感染に伴い  $\beta$  細胞が破壊され, 少数の自己反応性 T 細胞が活性化されても, 制御性 T 細胞による反応抑制以前に, 活性化 T 細胞応答は, いくつかの活性化後制御メカニズムにより, その過剰な反応は抑制されている。T 細胞の活性化後のアポトーシス誘導に働く分子としては, 既知の Fas に加えて programmed cell death-1 (PD-1) 抗原の重要性が強調されている。また, 細胞内シグナル伝達制御に関しては, suppressor of cytokine signaling (SOCS) などの分子が同定され, 将来の治療への応用も期待されている<sup>15)</sup>。さらに最近, 臨床的に 1 型糖尿病の発症早期に  $\beta$  細胞除去療法が有用であることが示され, 今後の展開が期待されている<sup>16,17)</sup> (図 2)。

#### おわりに

パンデミックと称されるほど, 世界的に増加している糖尿病は, 生活習慣の問題も含め, 様々な要因が蓄積されるため発症することを考えれば, ウイルス感染が環境因子として糖尿病誘発の危険因子の一つでありうることは想像に難くない。確かに, これまでの臨床的あるいは基礎的研究から, ウイルス感染が糖尿病の直接の原因あるいは間接的誘因であることは十分ありうると推測されるが, その証拠は乏しいのが現状である。もし, あるウイルスが糖尿病誘発の要因の一つであることが判明すれば, ワクチンによる予防が可能となるであろう。ただし, 現時点では, ウイルス感染を契機にして糖尿病を発症した症例について, ウイルス感染が原因であることを証明することは困難である。まず, 膵島細胞に親和性が高いウイルスを同定するような, ウイルスの糖尿病誘発性検定システムの開発が喫緊の課題であると考えられる。

- 1) 永淵正法: 糖尿病発症に関するウイルス感染症-糖尿病ウイルス原因説-. 月刊糖尿病 1(1): 144-151, 2009.
- 2) Vehik K, Dabelea D: The changing epidemiology of type 1 diabetes: why is it going through the roof? *Diabetes Metab Res Rev* 26: 2010, in press.
- 3) Jenson AB, Rosenberg HS, Notkins AL: Pancreatic islet-cell damage in children with fatal viral infections. *Lancet* 2: 354-358, 1980.
- 4) 今川彰久, 花房俊昭: 劇症 1 型糖尿病. 月刊糖尿病 1(6): 55-60, 2009.
- 5) Yoon JW: The role of viruses and environmental factors in the induction of diabetes. *Current Top Microbiol Immunol* 164: 95-123, 1990.
- 6) Kounoue E, Izumi K, Ogawa S *et al.*: The significance of T cells, B cells, antibodies and macrophages against encephalomyocarditis (EMC)-D virus-induced diabetes in mice. *Arch Virol* 153: 1223-1231, 2008.
- 7) Takeuchi O, Akira S: Innate immunity to virus infection. *Immunol Rev* 227: 75-86, 2009.
- 8) 永淵正法, 塚本 浩, 新納宏昭ほか: 自己免疫疾患と炎症. 細胞工学 29: 769-775, 2010.
- 9) 及川洋一, 島田 朗: インターフェロン治療と 1 型糖尿病. 臨床とウイルス 38: 2010, 印刷中
- 10) 永淵正法, 近藤しおり: 自己免疫性 1 型糖尿病とウイルス感染. *Diabetes Frontier* 21: 314-319, 2010.
- 11) Pak CY, Eun HM, McArthur RG *et al.*: Association of cytomegalovirus infection with autoimmune type 1 diabetes. *Lancet* 2: 1-4, 1988.
- 12) Nagamine K, Peterson P, Scott HD *et al.*: Positional cloning of the APECED gene. *Nat Genet* 17: 393-398, 1997.
- 13) Sakaguchi S: Naturally arising Foxp3-expressing CD25<sup>+</sup>CD4<sup>+</sup> regulatory T cells in immunological tolerance to self and non-self. *Nat Immunol* 6: 345-352, 2005.
- 14) Kogawa K, Kudoh J, Nagafuchi S *et al.*: Distinct clinical phenotype and immunoreactivity in Japanese siblings with autoimmune polyglandular syndrome type 1 (APS-1) associated with compound heterozygous novel AIRE gene mutations. *Clin Immunol* 103: 277-283, 2002.
- 15) Yoshimura A, Naka T, Kubo M: SOCS proteins, cytokine signalling and immune regulation. *Nat Rev Immunol* 7: 454-465, 2007.
- 16) Pescovitz MD, Greenbaum CJ, Krause-Steinrauf H *et al.*: Rituximab, B-lymphocyte depletion, and preservation of beta-cell function. *N Engl J Med* 361: 2143-2152, 2009.
- 17) Nagafuchi S, Katsuta H, Anzai K: Rituximab, B-lymphocyte depletion, and beta-cell function. *N Engl J Med* 362: 761, 2010.

## ウイルス感染の免疫防御と自己免疫

永淵正法, 栗崎宏憲, 勝田 仁 九州大学大学院 医学研究院 保健学部門

### 〔論文要旨〕

ウイルス感染症に対して、宿主は、まず物理的、化学的障壁、次に自然免疫、引き続いて、獲得免疫のメカニズムにより対抗している。このような防御機構は、いわゆる炎症をきたし、程度の差はあれ、しばしば組織障害をもたらすが、通常は、免疫応答の終息、組織修復機転により回復する。近年の免疫学の進歩は自然免疫における病原体のパターン認識機構（PAMPs：pathogen associated molecular patterns）、また、獲得免疫においては、ウイルスを始めとする細胞内寄生体に対抗する Th1 反応、寄生虫に対応する Th2 反応に加えて細胞外細菌に好中球応答を誘導する Th17 反応、さらに免疫応答制御に関する調節性 T 細胞（Treg）の存在を明らかにしてきた。免疫応答調節機構の破綻は、過剰な免疫反応による組織障害に関することも明らかとなってきた。さらにウイルス感染細胞が傷害され、免疫機序により排除されるメカニズムは、自己に対する反応でもあるため、ウイルス感染を契機として自己免疫反応が誘導されることは想像に難くない。幸い、生体は多くのシステムで自己応答の発生を多重に制御している。自己免疫疾患は、この制御機構の単一もしくは複数の障害が重なることで発症すると考えられる。ここでは、ウイルス感染防御機構について概説し、さらに自己免疫応答誘導機構とその制御について述べる。

### 1. はじめに

ウイルス感染に対しては、まず、皮膚、粘膜などの物理的障壁とそれぞれ汗腺、粘液、などの分泌物における病原体の洗浄、化学的障害による排除機構が働く（図1）。この第一線の障壁を突破すれば、いわゆる自然免疫が働く<sup>1)</sup>。近年の自然免疫に関する進歩は、病原体を非特異的に捕捉するのみでなく、パターンで判読するメカニズムの存在を明らかとしてきた。すなわち、それぞれの病原体について、進化の過程で保存されている pathogen-associated molecular patterns (PAMPs) を対象として認識する宿主の防御システムが存在している。その認識は、

パターン認識レセプター（pattern recognition receptors：PRRs）が行い、免疫シグナルを伝達することにより病原体に対抗する免疫応答の重要な位置を占めていることが明示されている。PRRs には、Toll-like receptors (TLRs), RNA helicase RIG-I-like receptors (RLRs), nucleotide-binding oligomerization domain-like receptors (NLRs), cytosolic DNA sensor などが知られている（図2）<sup>2)</sup>。

このような PRRs を介する経路はインターフェロン（図3）をはじめとするさまざまなサイトカイン応答を惹起し、ウイルスの増殖抑制に作用するとともにマクロファージを活性化し、ウイルスの貪食処理を担う。同時にこの応答はウイルス感染を契機とする場合、主として

Protective immunity against viral infection and autoimmune diseases

Seiho NAGAFUCHI, Hironori KURISAKI, Hitoshi KATSUTA, Department of Medical Science and Technology, Graduate School of Medical Sciences, Kyushu University

別刷請求先：永淵正法 〒812-8582 福岡市東区馬出3-1-1 九州大学大学院 医学研究院・保健学部門  
検査技術科学分野・病態情報学講座、九州大学院 内科  
Tel/Fax：092-642-6731 E-mail：nagafuchi@shs.kyushu-u.ac.jp

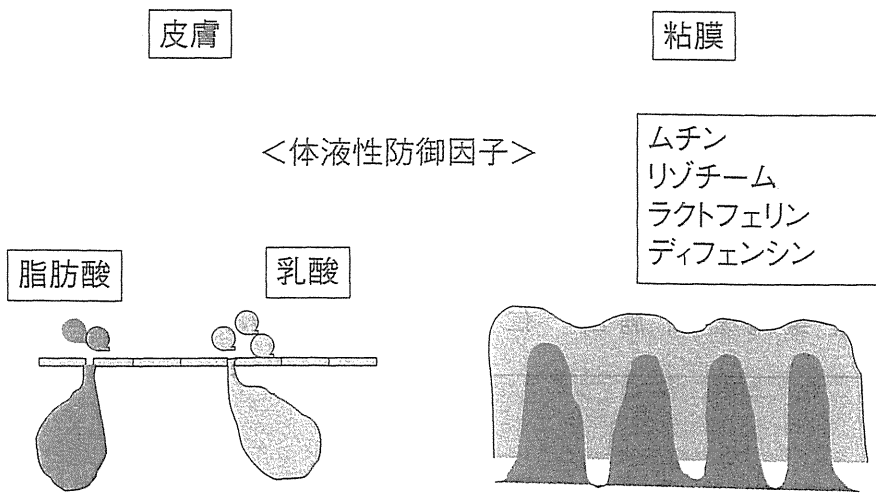


図1 生体防御の物理的, 化学的障壁

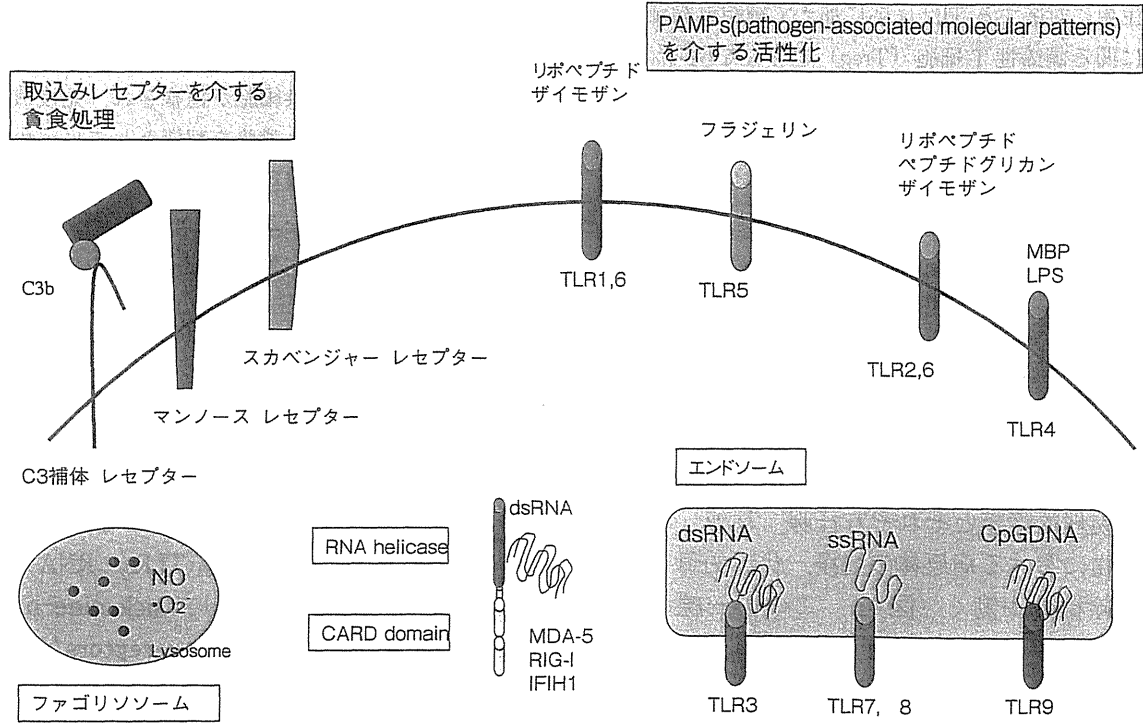


図2 自然免疫における非特異的および病原体パターン認識レセプター

IL-2により誘導される Th1反応を惹起することによりマクロファージの活性化, あるいは, 細胞傷害性 T細胞, IgG 抗体産生をもたらす(図4)<sup>3-5)</sup>. 補体は異物認識, レクチン経路による活性化, 抗体による活性化, ADCC(抗体依存性細胞媒介性細胞傷害)<sup>6)</sup>などを介して, エンベロープを有するウイルスの溶解反応, ウ

イルス感染細胞の破壊, あるいは炎症反応の惹起によるウイルス排除に作用する. このような免疫応答は, ウイルス感染が終息することによる抗原刺激の減少, 活性化された免疫系の抑制, 免疫調節機構による抑制などにより, 速やかに抑制され, 沈静化する.



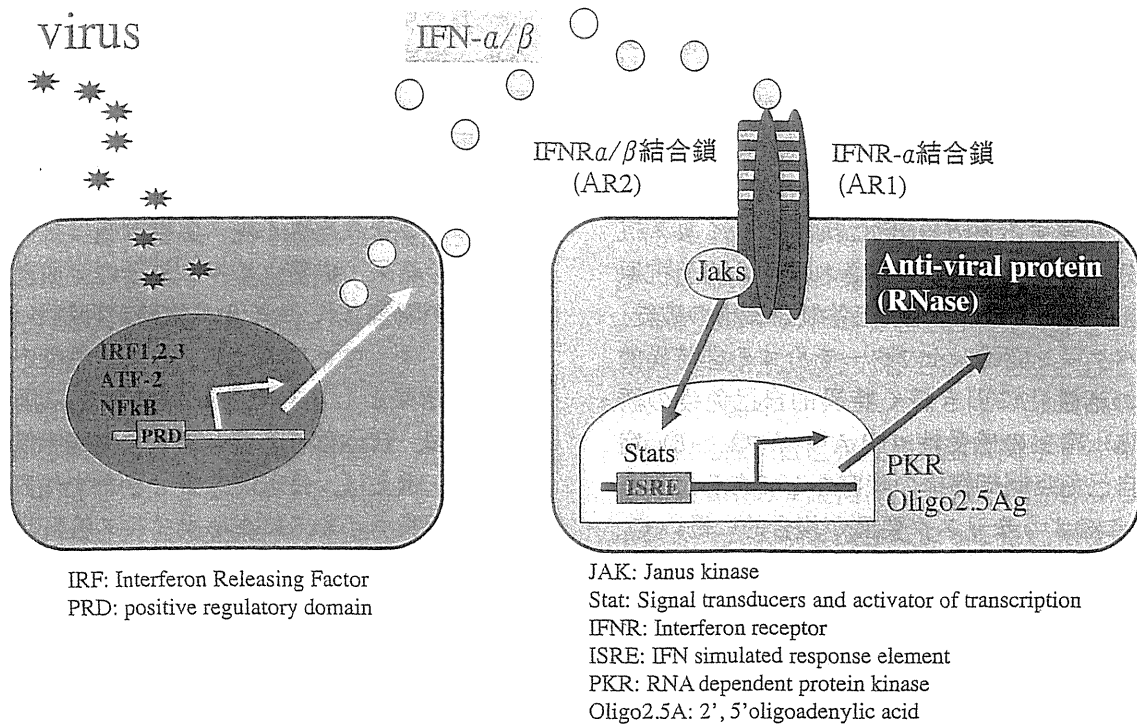


図3 インターフェロンの誘導と抗ウイルス活性の発揮

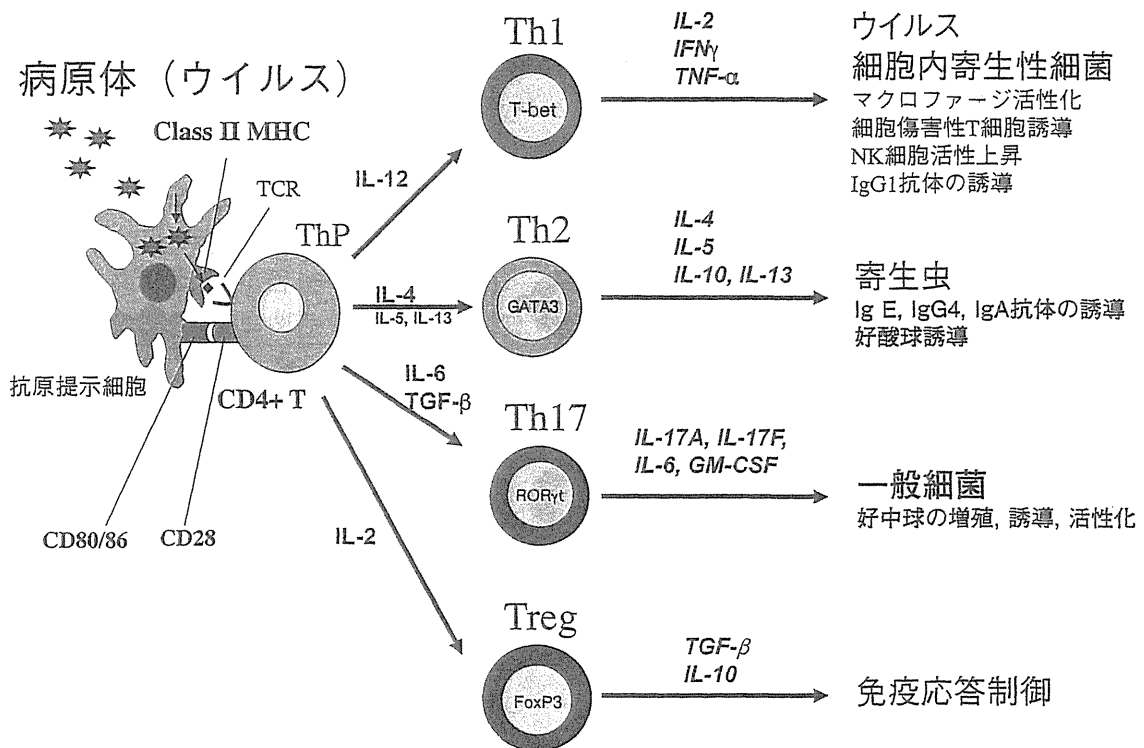


図4 生体防御システムにおける獲得免疫の種類とその意義

## 2. ウイルス感染による自己免疫糖尿病誘発あるいは抑制メカニズム

ウイルス感染が契機となって特異的自己免疫が誘導されるメカニズムにはいくつかの要因がある。列挙すると (1) 自己抗原とウイルス抗原の分子相同性、(2) 隠蔽されている自己抗原の表出誘導、(3) 自己免疫応答制御機構の破綻、(4) パターン認識レセプターを介する非特異的免疫の活性化に引き続く特異的自己免疫の誘導、(5) 宿主の感受性 (HLA タイプ)、(6) 宿主の自己免疫制御機構の障害などである。実際には、このようなりスク要因が複合的に働いて、自己免疫反応の誘導をもたらすのではないかと考えられる<sup>7,8)</sup>。

### I. 特異的自己免疫応答の活性化

#### (1) ウイルスと自己細胞抗原の分子相同性

ギラン・バレー症候群では、細菌である *Campylobacter jejuni* と、宿主の末梢神経 GM1 ganglioside の分子相同性を誘因として、その発症に関することは良く知られているが、ウイルス抗原と自己細胞抗原が交差することによる自己免疫応答惹起の直接の証拠は乏しい<sup>7,9)</sup>。

一方、ウイルスは、偏性細胞内寄生体であるため、増殖するためには、宿主の複製機能を必要とする。その過程で、初期の核酸合成酵素などの早期抗原 (Early Antigen) は細胞表面に表出され、ウイルス抗原特異的細胞傷害性 T 細胞の標的となり、ウイルス感染細胞は排除される。その結果、成熟ウイルス粒子の完成前に細胞機能が障害され、ウイルス増殖が抑制される。このことは、ウイルス抗原に対する免疫応答であるが結果として自己肝細胞の障害に働くため、一面、自己免疫応答と類似する臨床像を呈しうる。例えば、持続的感染をきたす代表疾患である肝炎ウイルスによるウイルス性肝炎、あるいは自己免疫性肝炎も肝臓細胞を傷害することにおいては同一の臨床像を呈し、その鑑別は困難である (図 5)。臨床的には自己抗体の有無が重要な鑑別点になるが、同時に存在し、合併と診断すべきかどうか苦慮する場合もある。サイトメガロウイルスの慢性感染に伴う自己免疫糖尿病の報告は興味深い<sup>10)</sup>。

#### (2) 自己抗原の遊離とその認識

前述したようにウイルス感染細胞の傷害により隠蔽されている自己抗原の表出誘導や自己抗原の遊離は、その後の自己反応性の惹起に働く

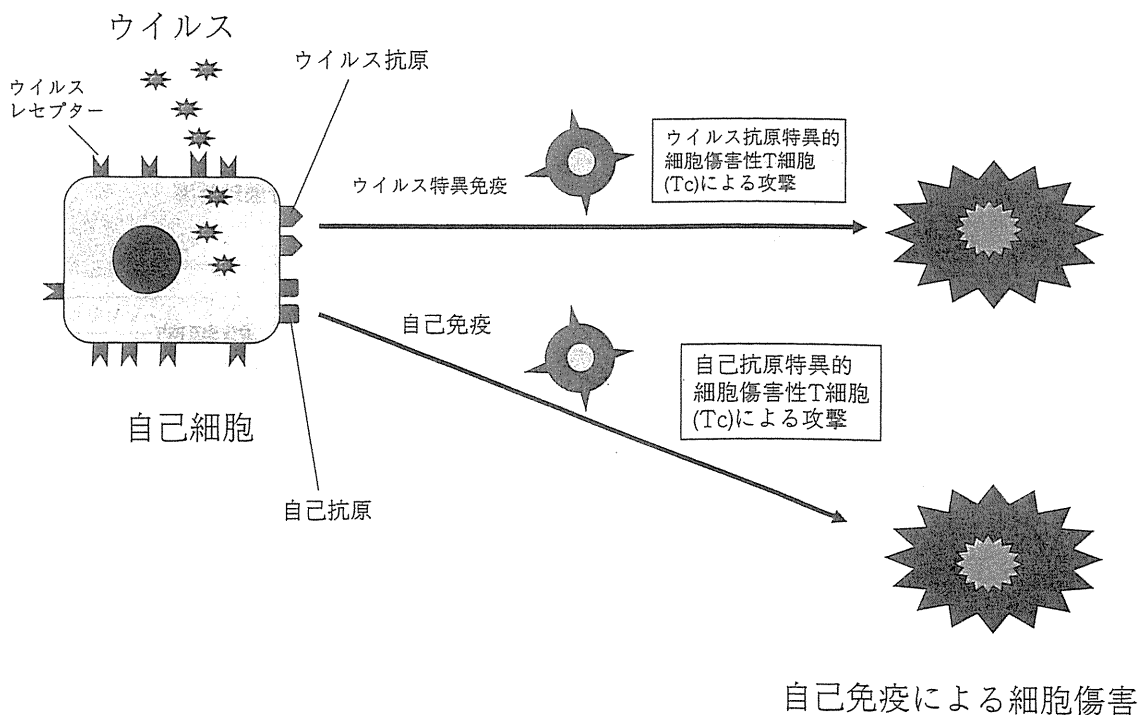


図5 ウイルス感染による細胞傷害と自己免疫の誘導

ことは容易に考えられる。そもそも自己反応性 T 細胞、あるいは B 細胞は、生体に少数であるが存在していることは良く知られているので、ウイルス感染細胞破溶解による自己抗原の提示により、このような非活性化状態の自己免疫反応が、より強く、かつ継続して活性化されることは充分にありうる。ただし、その場合、自己免疫応答制御機構の障害、あるいは破綻が伴って、はじめて自己免疫病の発症につながるであろう。

### (3) 自己免疫応答制御機構の破綻

自己反応性は、さまざまなメカニズムで制御されている。最近の免疫学のトピックとして、中枢性の自己免疫反応性 T 細胞の除去に働く自己免疫調節遺伝子 AIRE の同定と、末梢における自己反応性を制御する Foxp3<sup>+</sup> CD25<sup>+</sup> CD4<sup>+</sup> 調節性 T 細胞 (Treg) の発見は、この分野に目覚ましい進歩をもたらした<sup>11,12)</sup>。AIRE 欠損でもたらされる臓器特異的自己免疫の標的臓器は、一般に、副腎、副甲状腺が中心であるが<sup>13)</sup>、興味深いことに HLA タイプが 1 型糖尿病感受性であれば、1 型糖尿病を合併し、1 型糖尿病抵抗性では、むしろ典型的なアジソン病と副甲状腺機能低下の臨床像を呈する<sup>14)</sup>。一方、Treg の欠損では、むしろ 1 型糖尿病は主徴の 1 つである<sup>12)</sup>。このことは、自己免疫糖尿病発症制御には Treg による末梢性の免疫応答調節がより重要であることを示唆している。すなわち、自己免疫病の表現型には宿主の HLA、AIRE、Treg などの要因が複雑に関与することが示唆される。

一方、ウイルス感染に伴い  $\beta$  細胞が破壊され少数の自己反応 T 細胞が活性化されても、制御性 T 細胞による反応抑制以前に、活性化 T 細胞応答は、いくつかの活性化後制御メカニズムにより、その過剰な反応は抑制されている。T 細胞の活性化後のアポトーシス誘導に働く分子としては、既知の Fas に加えて programmed cell death-1 (PD-1) 抗原の重要性が強調されている<sup>7)</sup>。また、細胞内シグナル伝達制御に関しては、suppressor of cytokine signaling (SOCS) などの分子が同定され、将来の治療への応用も期待されている<sup>15)</sup>。さらに最近、種々の自己免疫疾患に B 細胞除去療法が有用であることが示

され、われわれが過去に報告した 1 型糖尿病に関する実験研究とともに、B 細胞による免疫応答調節の意義も注目されつつある(図 6)<sup>7,16-18)</sup>。

### (4) ウイルスによる自然免疫応答の活性化を介する自己免疫応答の誘導

従来、病原体から生体を守るシステムとしては、非特異的な病原体の取り込みと処理、インターフェロンの誘導などを自然免疫とし(図 2, 3)、特異的な免疫応答を獲得免疫として捉えていた(図 4)。

自然免疫が自己免疫病発症に関与するもっとも良い臨床的な証拠は、C 型肝炎治療のためのインターフェロン投与によって自己免疫糖尿病発症例が蓄積されていることであり、本誌で及川先生らが詳述されている<sup>19)</sup>。また、実験的にも、糖尿病抵抗性の BBR ラットは、Kilham rat virus 感染後、後述の病原体パターン認識機構である Toll-like receptor (TLR) 9 シグナルを介する自己免疫の誘導により、自己免疫糖尿病を発症する<sup>20)</sup>。最近、自然免疫に関する PPR のうち、IFIH1 (interferon induced helicase C, domain 1) の多型が 1 型糖尿病と関連あることが報告されている<sup>21)</sup>。この多型が感受性を決定するのか、あるいは抵抗性に関与するのかの詳細は今後の研究課題であろう。

## II. 自己免疫誘導の抑制

ウイルス感染がむしろ自己免疫の発症を抑制することがありうることは旧くから知られていた<sup>22)</sup>。最近、Filippi らは、Coxsackie B3 ウイルスあるいは lymphocytic choriomeningitis virus (LCMV) を自己免疫糖尿病モデル動物である NOD マウスに感染させたところ糖尿病の発症が遅延し、その原因として、リンパ球における programmed cell death-1 ligand 1 (PD-L1) の発現が上昇することによる PD-1 表出 CD8 陽性細胞傷害性 T 細胞の増殖抑制に加えて、CD4<sup>+</sup> CD25<sup>+</sup> Treg の増加がもたらされるとする興味深い研究を報告している<sup>23)</sup>。すなわち、本研究は、ウイルス感染が調節性 T 細胞を障害することにより、1 型糖尿病が誘発されるリスクが存在する一方、調節性 T 細胞を増加させることにより 1 型糖尿病発症を阻止しうることを示しており、ウイルス感染が宿主免疫機構に及ぼす影響

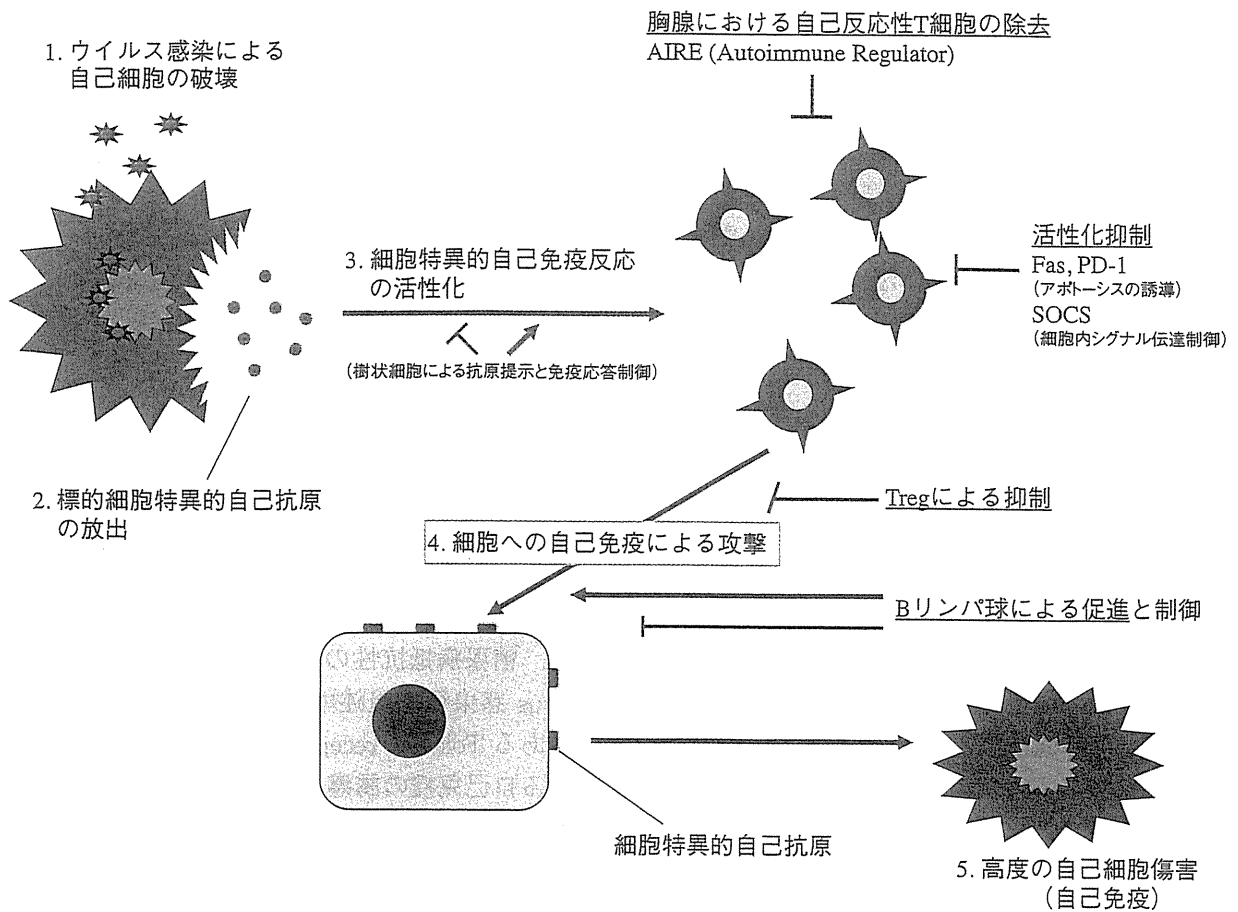


図6 ウイルス感染による自己免疫の誘導とその制御機構

の多面性を理解する上でも興味深い知見である。

### 3. おわりに

ウイルス感染と自己免疫病の関連は、充分ありうるものの、その直接の証拠は乏しいのが現状である。もし、あるウイルスが自己免疫病の原因であることが判明すればワクチンによる自己免疫疾患の予防が可能となるであろう。ただし、現時点では、自己免疫疾患の症例について、ウイルス感染を契機として発症したことを証明することは困難である。そもそも、本稿で述べて来たように、自己免疫応答は多くのメカニズムで、多重に制御されている。ウイルス感染によって惹起された自己免疫応答が制御され、終息するのか、あるいは、臨床的な自己免疫につながるのかは、さまざまな免疫制御メカニズム、感受性要因が複合して関与するのではないかと推測される (図6)。ただし、ウイルスが自己細胞に感染することが自己免疫反応誘導のトリ

ガーとなりうることは疑いの余地がない。今後の研究の進展がウイルス感染と自己免疫病の関連の全貌を明らかにすることを期待したい。

### 参考文献

- 1) 永淵正法 : 感染症成立の背景解析とその対策. 日本皮膚科学会雑誌 117 : 759-765, 2007
- 2) Takeuchi O, Akira S : Innate immunity to virus infection. Immunol Rev 227 : 75-86, 2009
- 3) Komatsu T, Ireland DD, Reiss CS : IL-12 and viral infection. Cytokine Growth Fact Rev 9 : 277-285, 1998
- 4) Nagafuchi S, Oda H, Mori R, Taniguchi T : Mechanism of acquired resistance to herpes simplex virus infection as studied in nude mice. J gen Virol 44 : 715-723, 1979
- 5) Nagafuchi S, Hayashida I, Higa K, Wada T, Mori R : Role of Lyt-1 positive immune T cells in recovery from herpes simplex virus infection in mice.

- Microbiol Immunol 26 : 359-362, 1982
- 6) Hayashida I, Nagafuchi S, Hayashi Y, Kino Y, Mori R, Oda H, Ohtomo N, Tashiro A : Mechanism of antibody mediated protection against herpes simplex virus infection in mice : Requirement of Fc portion of antibody. Microbiol Immunol 26 : 497-509, 1982
  - 7) 永淵正法, 塚本 浩, 新納宏昭, 小林隆志 : 自己免疫疾患と炎症. 細胞工学 29(9) : 769-775, 2010
  - 8) Chervonsky AV : Influence of microbial environment on autoimmunity. Nat Immunol 11 : 28-33, 2010
  - 9) Christen U, Hintermann E, Holdener M, von Herrath MG : Viral triggers for autoimmunity : Is the "glasso molecular mimicry" half full or half empty? J Autoimmu 34 : 38-44, 2010
  - 10) Pak CY, Eun HM, McArthur RG, Yoon JW : Association of cytomegalovirus infection with autoimmune type 1 diabetes. Lancet 2 : 1-4, 1988
  - 11) Nagamine K, Peterson P, Scott HS, Kudoh J, Minoshima S, Heino M, Krohn KJ, Laloti MD, Mullis PE, Antonarakis SE, Kawasaki K, Asakawa S, Ito F, Shimizu N : Positional cloning of the APECED gene. Nat Genet 17 : 393-398, 1997
  - 12) Sakaguchi S : Naturally arising Foxp3-expressing CD25<sup>+</sup> CD4<sup>+</sup> regulatory T cells in immunological tolerance to self and non-self. Nat Immunol 6 : 345-352, 2005
  - 13) Eisenbarth GS, Gottlieb PA : Autoimmune polyendocrine syndromes. N Engl J Med 350 : 2068-2079, 2004
  - 14) Kogawa K, Kudoh J, Nagafuchi S, Ohga S, Katsuta H, Ishibashi H, Harada M, Hara T, Shimizu N : Distinct clinical phenotype and immunoreactivity in Japanese siblings with autoimmune polyglandular syndrome type 1 (APS-1) associated with compound heterozygous novel AIRE gene mutations. Clin Immunol 103 : 277-283, 2002
  - 15) Yoshimura A, Naka T, Kubo M : SOCS proteins, cytokine signalling and immune regulation. Nat Rev Immunol 7 : 454-65, 2007
  - 16) Dörner T, Radbruch A, Burmester GR : B-cell-directed therapies for autoimmune disease. Nat Rev Rheumatol 5, 433-441, 2009
  - 17) Nagafuchi S, Katsuta H, Anzai K : Rituximab, B-lymphocyte depletion, and beta-cell function. N Engl J Med 362 : 761, 2010
  - 18) Nagafuchi S : The role of B cells in regulating the magnitude of immune response. Microbiol Immunol 54 : 487-490, 2010
  - 19) 及川洋一, 島田 朗 : インターフェロンと1型糖尿病 臨床とウイルス 39(1) : 10-19, 2011
  - 20) Zipris D, Lien E, Nair A, Xie JX, Greiner DL, Mordes JP, Rossini AA : TLR9-signalling pathways are involved in Kilham rat virus-induced autoimmune diabetes in the biobreeding diabetes-resistant rat. J Immunol 178 : 693-701, 2007
  - 21) Smyth DJ, Cooper JD, Bailey R, Field S, Burren O, Smink LJ, Guja C, Ionescu-Tirgoviste C, Widmer B, Dunger DB, Savage DA, Walker NM, Clayton DG, Todd JA : A genome-wide association study of nonsynonymous SNPs identifies a type 1 diabetes locus in the interferon-induced helicase (*IFIH1*) region. Nat Genet 38 : 617-619, 2006
  - 22) Oldstone MB : Prevention of type 1 diabetes in nonobese diabetic mice by virus infection, Science 239 : 500-502, 1988
  - 23) Filippi CM, Estes EA, Oldham JE, von Herrath MG : Immunoregulatory mechanisms triggered by viral infections protect from type 1 diabetes in mice. J Clin Invest 119 : 1515-1523, 2009

## R723, a selective JAK2 inhibitor, effectively treats JAK2V617F-induced murine myeloproliferative neoplasm

\*Kotaro Shide,<sup>1</sup> Takuro Kameda,<sup>1</sup> \*Vadim Markovtsov,<sup>2</sup> Haruko K. Shimoda,<sup>1</sup> Elizabeth Tonkin,<sup>2</sup> Shuling Fang,<sup>2</sup> Chian Liu,<sup>2</sup> Marina Gelman,<sup>2</sup> Wayne Lang,<sup>2</sup> Jason Romero,<sup>2</sup> John McLaughlin,<sup>2</sup> Somasekhar Bhamidipati,<sup>2</sup> Jeffrey Clough,<sup>2</sup> Caroline Low,<sup>2</sup> Andrea Reitsma,<sup>2</sup> Stacey Siu,<sup>2</sup> Polly Pine,<sup>2</sup> Gary Park,<sup>2</sup> Allan Tomeros,<sup>2</sup> Matt Duan,<sup>2</sup> Rajinder Singh,<sup>2</sup> Donald G. Payan,<sup>2</sup> Takuya Matsunaga,<sup>1</sup> Yasumichi Hitoshi,<sup>2</sup> and Kazuya Shimoda<sup>1</sup>

<sup>1</sup>Department of Gastroenterology and Hematology, Faculty of Medicine, Miyazaki University, Kiyotake, Miyazaki, Japan, and <sup>2</sup>Rigel Pharmaceuticals Inc, San Francisco, CA

The activating mutations in JAK2 (including JAK2V617F) that have been described in patients with myeloproliferative neoplasms (MPNs) are linked directly to MPN pathogenesis. We developed R723, an orally bioavailable small molecule that inhibits JAK2 activity in vitro by 50% at a concentration of 2nM, while having minimal effects on JAK3, TYK2, and JAK1 activity. R723 inhibited cytokine-independent CFU-E growth and constitu-

tive activation of STAT5 in primary hematopoietic cells expressing JAK2V617F. In an anemia mouse model induced by phenylhydrazine, R723 inhibited erythropoiesis. In a leukemia mouse model using Ba/F3 cells expressing JAK2V617F, R723 treatment prolonged survival and decreased tumor burden. In V617F-transgenic mice that closely mimic human primary myelofibrosis, R723 treatment improved survival, hepatosplenomegaly, leukocytosis,

and thrombocytosis. R723 preferentially targeted the JAK2-dependent pathway rather than the JAK1- and JAK3-dependent pathways in vivo, and its effects on T and B lymphocytes were mild compared with its effects on myeloid cells. Our preclinical data indicate that R723 has a favorable safety profile and the potential to become an efficacious treatment for patients with JAK2V617F-positive MPNs. (*Blood*. 2011;117(25):6866-6875)

### Introduction

Myeloproliferative neoplasms (MPNs) are clonal hematologic diseases characterized by excess production of one or more lineages of mature blood cells, resulting in a predisposition to bleeding and thrombosis, extramedullary hematopoiesis (EMH), and a progression to acute leukemia.<sup>1</sup> A somatic activating mutation encoding a valine to phenylalanine substitution at position 617 (V617F) in JAK2 was discovered as a common molecular marker in Philadelphia chromosome-negative MPNs.<sup>2-5</sup> The incidence of the JAK2V617F mutation is found in > 90% of patients with polycythemia vera (PV) and affects approximately half of the patients with essential thrombocythemia (ET) and primary myelofibrosis (PMF). Expression of JAK2V617F in vivo in a murine BM transplantation assay resulted in erythrocytosis resembling PV.<sup>6-8</sup> Moreover, we and others have reported that JAK2V617F-transgenic (V617F-TG) mice develop 3 kinds of MPNs: PV like, ET like, and PMF like.<sup>9-11</sup> These studies support a critical role for JAK2V617F in the pathogenesis of the 3 types of MPNs.

Current therapy for MPNs<sup>12-14</sup> is empirically derived and includes phlebotomy,<sup>15</sup> hydroxyurea,<sup>16</sup> IFN- $\alpha$ ,<sup>17</sup> anagrelide,<sup>16</sup> and thalidomide<sup>18</sup> and its analogs.<sup>19</sup> Most patients are not candidates for stem-cell transplantation, which is the curative treatment for MPNs,<sup>20</sup> given their advanced age at the time of diagnosis, considerably high ratio of transplantation-related mortality, and relatively indolent progression. Identification of specific JAK2 inhibitors appears to be an important step toward the development

of targeted therapy for MPNs. Several groups of investigators have begun to develop specific, potent, orally bioavailable JAK2 inhibitors for the treatment of MPNs,<sup>21-24</sup> and these compounds are currently undergoing clinical trials.<sup>25-27</sup>

In the present study, we report the development of R723, a selective small-molecule JAK2 inhibitor. We show that R723 is a potent inhibitor of JAK2V617F in cell-based assays. In 3 mouse models, R723 had significant in vivo activity against JAK2V617F, was well tolerated, and had a minimal impact on T- and B-cell numbers.

### Methods

#### Materials

Cell lines, the JAK2V617F clone, and vectors are described in supplemental Methods (available on the *Blood* Web site; see the Supplemental Materials link at the top of the online article).

#### Identification of JAK2 inhibitors

To identify JAK2 inhibitors, we used a cell-based approach using murine leukemia Ba/F3 cells expressing JAK2V617F with the erythropoietin (EPO) receptor Ba/F3-EPOR-JAK2V617F. Initially, we screened a focused, diversified kinase inhibitor library to identify inhibitors of Ba/F3-EPOR-JAK2V617F cell proliferation. To avoid nonselective compounds targeting other members of the JAK family and molecules with general toxicity, we

Submitted January 3, 2010; accepted April 15, 2011. Prepublished online as *Blood* First Edition paper, April 29, 2011; DOI 10.1182/blood-2010-01-262535.

\*K.S. and V.M. contributed equally to this study.

The online version of this article contains a data supplement.

The publication costs of this article were defrayed in part by page charge payment. Therefore, and solely to indicate this fact, this article is hereby marked "advertisement" in accordance with 18 USC section 1734.

© 2011 by The American Society of Hematology

used 2 additional assays assessing the effects on IL-2–dependent proliferation of human primary T lymphocytes, CTLL-2 mouse T-cell leukemia cells, and JAK1-dependent Ba/F3 cells expressing JAK1V658F. The use of these counterscreen assays also allowed us to exclude the possibility of cell-type- and species-specific artifacts. R723 was obtained as a result of the systemic chemical modification of the initial hits, followed by testing of the resulting compounds in the assays mentioned above.

### In vitro proliferation assays

The half-maximal inhibitory concentration ( $IC_{50}$ ) for the inhibition of proliferation of all the cell lines was determined using CellTiter-Glo Luminescent Cell Viability Assay reagent (Promega). For details, see supplemental Methods.

### Cell-based STAT5 phosphorylation assay

Effects of R723 on STAT5 phosphorylation in human primary T cells and cell lines were determined by FACS. For details, see supplemental Methods.

### Animals

Eight-week-old female BALB/c mice and 7-week-old female NOD/SCID mice (The Jackson Laboratory) were used in the induced hemolytic anemia model and PK-PD studies and in the Ba/F3-JAK2V617F leukemia study, respectively. Two lines of V617F-TG mice were established and analyzed as described previously.<sup>9</sup> In this experiment, we used line 2 mice that showed the spectrum of clinicopathologic features of human PMF.<sup>9</sup> Animal studies were performed in the United States in accordance with the Institutional Animal Care and Use Committee of Rigel Pharmaceuticals Inc, and in Japan in accordance with the Miyazaki University Ethics Committee.

### Analysis of JAK2- and JAK1/JAK3-dependent STAT5 phosphorylation in primary cells

Wild-type (WT) mice (female BALB/c) were dosed orally with R723 at 50 or 100 mg/kg or vehicle, and blood was collected at 1 and 3 hours after treatment. After stimulation with either 10 ng/mL of GM-CSF for the assessment of JAK2 activity in granulocytes ( $Gr-1^+$ ) or 100 ng/mL of IL-15 for the assessment of JAK1/JAK3 activity in T cells ( $CD8^+$ ), the cells were fixed and permeabilized and then stained with Alexa Fluor 647–conjugated pSTAT5 and either PE-conjugated Gr-1 or peridinin chlorophyll A protein–cyanin 5.5–conjugated CD8. Samples were analyzed by FACS.

### PHZ-induced hemolytic anemia model and Ba/F3-JAK2V617F engraftment mouse model

Phenylhydrazine (PHZ; Sigma-Aldrich) was administered at 50 mg/kg/d intraperitoneally for 2 consecutive days to deplete RBCs and to stimulate erythropoiesis. R723 formulated in 0.1% hydroxypropyl methylcellulose was administered by oral gavage starting the day after the final PHZ administration (day 2). R723 dosing continued through day 7 at 50 mg/kg or 75 mg/kg twice daily. Blood was collected on days 3, 6, and 8 to assess RBC number and hematocrit levels. The Ba/F3-JAK2V617F engraftment mouse model is described in supplemental Methods.

### Murine MPN model and analysis of mice after R723 treatment

Twelve-week-old V617F-TG mice were treated by oral gavage twice daily with 35 mg/kg R723, 70 mg/kg R723, or vehicle for 16 weeks. In this study, a salt form of R723 was formulated in water to ease the formulation process. As a control for V617F-TG treated with vehicle, we prepared WT mice treated with vehicle. Differential blood counts were assessed by retro-orbital eye bleeds before study initiation, during the study, and at the end of the study. Mice were killed at the study end point. For pathologic examination, tissue samples were fixed in formalin, embedded in paraffin blocks, and sectioned for H&E staining or Gomori silver staining. FACS was performed as described previously.<sup>9</sup>

### V617F-TG BM cell engraftment mouse model

BM cells ( $2$  to  $8 \times 10^6$ ) from  $CD45.2^+$  V617F-TG mice, together with  $2 \times 10^5$   $CD45.1^+$  WT BM cells, were injected into 9.5 Gy–irradiated recipient  $CD45.2^+$  WT mice. In our preliminary experiments, we injected  $2 \times 10^6$   $CD45.1$  BM cells into lethally irradiated (9.5 Gy)  $CD45.2$  recipients. Reconstitution of recipients with donor BM cells was monitored by assessing the frequency of  $CD45.1^+/CD45.2^+$  cells in the peripheral blood (PB) after transplantation. Twelve weeks after the transplantation, donor-derived ( $CD45.1$ ) cells had nearly completely replaced (99%) the recipient ( $CD45.2$ ) cells in the PB. The remaining recipient cells in PB were 1%. Therefore, under the conditions of our cotransplantation experiments, nearly all of the  $CD45.2^+$  cells in the PB were derived from V617F-TG. Twenty weeks after BM transplantation, recipient mice were divided into R723 treatment or vehicle control groups. R723 was administered by oral gavage at 70 mg/kg twice daily for 4 weeks, whereas the control group received vehicle only. Complete blood counts and the ratio of  $CD45.1^+$  to  $CD45.2^+$  cells were monitored by FACS before and after treatment. All mice were killed at study end points and spleens were weighed.

### Progenitor cell assays

Colony forming assays were performed as described previously<sup>9</sup> (for details, see supplemental Methods). CFU-E colonies were counted on day 3 and other colonies were counted on day 7. To observe the effect of R723 on the proportion of progenitors, V617F-TG mice were dosed orally with R723 at 70 mg/kg or vehicle twice daily for 4 weeks.  $Lin^-Sca-1^-cKit^+$  (LSK), common myeloid progenitor (CMP), granulocyte-macrophage progenitor (GMP), erythromegakaryocyte progenitor (MEP), megakaryocyte progenitor (MKP), early erythroblast, and late erythroblast populations in BM cells were determined by FACS. Antibodies were used as indicated in supplemental Methods.

### Statistical analysis

Results are presented as means  $\pm$  SE. To assess the statistical significance between the 2 groups, the 2-tailed Student *t* test was used. Statistical analyses of R723-treated groups versus vehicle groups in survival studies were performed with the log-rank test.

## Results

### R723 is a potent selective JAK2 inhibitor

To identify JAK2 inhibitors, we used a cell-based approach using murine leukemia Ba/F3 cells expressing JAK2V617F with the EPO receptor Ba/F3-EPOR-JAK2V617F. R723 was obtained as a potent and selective inhibitor of Ba/F3-EPOR-JAK2V617F proliferation through a screening of a focused, diversified kinase inhibitor library and through the structure-activity relationship study on the initial hits from the screening. The chemical structure of R723 and the crystal structure of R723 complexed with JAK2 catalytic domain are shown in supplemental Figure 1 (US Patent Application Pub. No. 2009-0258864 A1, October 15, 2009). R723 strongly suppressed proliferation of Ba/F3-EPOR-JAK2V617F and 2 other cell lines dependent solely on JAK2V617F signaling for survival: UKE-1 and SET-2.<sup>28</sup> R723 strongly diminished JAK2-dependent STAT5 phosphorylation in these cells (Table 1 and supplemental Figure 2A). R723 potentially targeted WT JAK2 activity, as indicated by the inhibition of EPO-driven proliferation of human  $CD34^+$ -derived erythroid progenitors. We then compared the ability of R723 to inhibit WT JAK2-dependent proliferation of Ba/F3-EPOR cells in the presence of EPO with that of JAK2V617F-dependent (and cytokine-independent) proliferation of Ba/F3-EPOR-JAK2V617F cells. Both cell lines were inhibited equally well by the compound, showing the lack of R723 selectivity between WT

**Table 1. R723 activity in cell-based assays**

Assay	Target	IC <sub>50</sub> , nM
Ba/F3-EPOR-JAK2V617F proliferation	JAK2 V617F	191
UKE1 proliferation	JAK2 V617F	168
SET2 proliferation	JAK2 V617F	139
EPO-dependent human CD34 <sup>+</sup> progenitor proliferation	JAK2	124
Ba/F3-EPOR-JAK2V617F pSTAT5 FACS	JAK2 V617F	390
SET2 pSTAT5 FACS	JAK2 V617F	39
IL-2 CTLL2 proliferation	JAK1/JAK3	528
IL-2 human primary T-cell proliferation	JAK1/JAK3	1260
IL-2 CTLL2 pSTAT5 FACS	JAK1/JAK3	2300
IL-2 human primary T-cell pSTAT5 FACS	JAK1/JAK3	2700
Ba/F3-JAK1V658F proliferation	JAK1 V658F	885
CMK proliferation	JAK3 A572V	2340
A549 proliferation	Multiple	3680
H1299 proliferation	Multiple	4100
IgE CHMC tryptase	Syk	760
Insulin HeLa pAKT in cell western	InsR	10 800
VEGF HUVEC pVEGFR in cell western	VEGFR	3250

and mutant forms of the enzyme in cells (supplemental Figure 2B). This observation agrees with the in vitro kinase inhibition data, in which no differences between the 2 were found (supplemental Table 1).

Characterization of R723 included a variety of cell-based assays probing multiple pathways (summarized in Table 1). The effects of R723 on the key off-target assays, IL-2-dependent proliferation and STAT5 phosphorylation via JAK1/JAK3 in human primary T lymphocytes and CTLL-2 cells, were significantly lower than the effects observed in the JAK2-dependent cell lines (Table 1). We also used a Ba/F3 cell line expressing the V658F mutant of JAK1 kinase (Ba/F3-JAK1V658F cells), which demonstrates IL3-independent but JAK1-dependent growth,<sup>29</sup> and the CMK cell line, which is dependent on the constitutively active JAK3A572V mutant, for survival and proliferation assays.<sup>30</sup> Both cell lines were weakly affected by R723. We observed moderate inhibition of Syk kinase activity, leading to a suppression of IgE-stimulated tryptase release in human mast cells. This effect, however, became pronounced only at a concentration higher than the one required for efficient inhibition of the JAK2-dependent pathway.

#### Biochemical selectivity of R723

As expected from the results of the cell-based assays, R723 was shown to be an extremely potent JAK2 inhibitor, with a biochemical IC<sub>50</sub> of 2nM (Table 2). It had a nearly identical inhibition profile

**Table 2. R723 selectively inhibits JAK2**

Kinase	IC <sub>50</sub> , nM	Selectivity over JAK2, -fold
JAK2	2	NA
JAK1	740	370
JAK3	26	13
TYK2	3950	> 500
VEGFR2	1400	> 500
Syk	300	150
PKCa	3960	> 500
PKCb1	7990	> 500
PKCd	> 10 000	> 500
PKCe	> 10 000	> 500
PKCq	> 10 000	> 500
PLK1	> 10 000	> 500
RET	109	55

for both the WT and the V617F mutant of JAK2 in a 2-point in vitro kinase assay (supplemental Table 1). R723 demonstrated good selectivity against all other JAK family kinases when tested at a wide range of concentrations. Selectivity ratios for IC<sub>50</sub> varied from 13-fold for JAK3 to a few hundred-fold for 2 other members of the family, JAK1 and Tyk2 (Table 2). The R723 selectivity was further confirmed by 2-point testing against a full panel of more than 200 enzymes. Only 13 other kinases cleared a threshold of 30% inhibition at 100nM, with the majority of them failing to show any discernable inhibition at 20nM, a concentration that is 10-fold higher than the JAK2 IC<sub>50</sub> (supplemental Table 1). These results indicate that R723 is a highly potent and selective JAK2 inhibitor in vitro.

#### R723 demonstrates selectivity in primary cells

R723 is an orally bioavailable compound demonstrating excellent pharmacokinetic properties in mice, making it a good candidate for in vivo testing (supplemental Figure 3). To assess the effects of R723 on JAK2 and JAK1/JAK3 signaling in vivo, we measured STAT5 phosphorylation in whole blood obtained from R723-treated WT mice (female BALB/c) on ex vivo stimulation of either Gr-1<sup>+</sup> granulocytes with GM-CSF or CD8<sup>+</sup> T cells with IL-15, respectively. Whereas the GM-CSF-mediated signaling cascade relied exclusively on JAK2, IL-15-dependent stimulation of T cells required both JAK1 and JAK3 activities. Both 50 and 100 mg/kg doses of R723 induced strong inhibition of STAT5 phosphorylation after GM-CSF and, to a lesser extent, IL-15 stimulation, especially when a 50 mg/kg dose of R723 was administered (Figure 1A). We consistently observed a preference for targeting the JAK2-dependent GM-CSF pathway, especially at the 50 mg/kg dose 1 hour after dosing.

#### R723 inhibits erythropoiesis in a PHZ-induced hemolytic anemia model

To investigate the ability of R723 to inhibit JAK2 in vivo, we used the acute mouse model based on induction of anemia on PHZ treatment.<sup>31</sup> PHZ-induced RBC damage and sequential depletion lead to hyperstimulation of normal and EMH accompanied by transient splenomegaly, followed by quick (7-10 days) recovery to normal hematocrit levels. As expected, 3 days after the first PHZ injection, both hematocrit and RBC values in all groups dropped to an average of 66% and 64% of naive controls, respectively. On days 6 and 8, however, progressive recovery was observed in vehicle control animals, whereas animals administered R723 showed a dose-dependent and significant ( $P < .05$ ) delay in recovery (Figure 1B), with the 75 mg/kg twice daily dose producing the strongest effect on both parameters ( $P < .01$ ).

#### R723 is effective in an acute Ba/F3-JAK2V617F leukemia model

We investigated the effect of R723 in a mouse leukemia model relying on the use of murine Ba/F3 cells expressing JAK2V617F as a driver of cell proliferation. This model is particularly aggressive, with a lethal outcome within 15 days of cell injection in vehicle-treated mice. In the R723-treated group, we observed a small (2 days, 13%) but highly significant improvement in survival ( $P < .004$ ) compared with the vehicle-treated cohort (supplemental Figure 4). In another study, animals were killed on day 13, before the full disease onset, to evaluate the levels of green fluorescent protein-positive (GFP<sup>+</sup>) Ba/F3-JAK2V617F cells in the spleen and BM. We observed a significant decrease in spleen cellularity and in



**Table 1. R723 activity in cell-based assays**

Assay	Target	IC <sub>50</sub> , nM
Ba/F3-EPOR-JAK2V617F proliferation	JAK2 V617F	191
UKE1 proliferation	JAK2 V617F	168
SET2 proliferation	JAK2 V617F	139
EPO-dependent human CD34 <sup>+</sup> progenitor proliferation	JAK2	124
Ba/F3-EPOR-JAK2V617F pSTAT5 FACS	JAK2 V617F	390
SET2 pSTAT5 FACS	JAK2 V617F	39
IL-2 CTLL2 proliferation	JAK1/JAK3	528
IL-2 human primary T-cell proliferation	JAK1/JAK3	1260
IL-2 CTLL2 pSTAT5 FACS	JAK1/JAK3	2300
IL-2 human primary T-cell pSTAT5 FACS	JAK1/JAK3	2700
Ba/F3-JAK1V658F proliferation	JAK1 V658F	885
CMK proliferation	JAK3 A572V	2340
A549 proliferation	Multiple	3680
H1299 proliferation	Multiple	4100
IgE CHMC tryptase	Syk	760
Insulin HeLa pAKT in cell western	InsR	10 800
VEGF HUVEC pVEGFR in cell western	VEGFR	3250

and mutant forms of the enzyme in cells (supplemental Figure 2B). This observation agrees with the *in vitro* kinase inhibition data, in which no differences between the 2 were found (supplemental Table 1).

Characterization of R723 included a variety of cell-based assays probing multiple pathways (summarized in Table 1). The effects of R723 on the key off-target assays, IL-2-dependent proliferation and STAT5 phosphorylation via JAK1/JAK3 in human primary T lymphocytes and CTLL-2 cells, were significantly lower than the effects observed in the JAK2-dependent cell lines (Table 1). We also used a Ba/F3 cell line expressing the V658F mutant of JAK1 kinase (Ba/F3-JAK1V658F cells), which demonstrates IL-3-independent but JAK1-dependent growth,<sup>29</sup> and the CMK cell line, which is dependent on the constitutively active JAK3A572V mutant, for survival and proliferation assays.<sup>30</sup> Both cell lines were weakly affected by R723. We observed moderate inhibition of Syk kinase activity, leading to a suppression of IgE-stimulated tryptase release in human mast cells. This effect, however, became pronounced only at a concentration higher than the one required for efficient inhibition of the JAK2-dependent pathway.

#### Biochemical selectivity of R723

As expected from the results of the cell-based assays, R723 was shown to be an extremely potent JAK2 inhibitor, with a biochemical IC<sub>50</sub> of 2nM (Table 2). It had a nearly identical inhibition profile

**Table 2. R723 selectively inhibits JAK2**

Kinase	IC <sub>50</sub> , nM	Selectivity over JAK2, -fold
JAK2	2	NA
JAK1	740	370
JAK3	26	13
TYK2	3950	> 500
VEGFR2	1400	> 500
Syk	300	150
PKCa	3960	> 500
PKCb1	7990	> 500
PKCd	> 10 000	> 500
PKCe	> 10 000	> 500
PKCq	> 10 000	> 500
PLK1	> 10 000	> 500
RET	109	55

for both the WT and the V617F mutant of JAK2 in a 2-point *in vitro* kinase assay (supplemental Table 1). R723 demonstrated good selectivity against all other JAK family kinases when tested at a wide range of concentrations. Selectivity ratios for IC<sub>50</sub> varied from 13-fold for JAK3 to a few hundred-fold for 2 other members of the family, JAK1 and Tyk2 (Table 2). The R723 selectivity was further confirmed by 2-point testing against a full panel of more than 200 enzymes. Only 13 other kinases cleared a threshold of 30% inhibition at 100nM, with the majority of them failing to show any discernable inhibition at 20nM, a concentration that is 10-fold higher than the JAK2 IC<sub>50</sub> (supplemental Table 1). These results indicate that R723 is a highly potent and selective JAK2 inhibitor *in vitro*.

#### R723 demonstrates selectivity in primary cells

R723 is an orally bioavailable compound demonstrating excellent pharmacokinetic properties in mice, making it a good candidate for *in vivo* testing (supplemental Figure 3). To assess the effects of R723 on JAK2 and JAK1/JAK3 signaling *in vivo*, we measured STAT5 phosphorylation in whole blood obtained from R723-treated WT mice (female BALB/c) on *ex vivo* stimulation of either Gr-1<sup>+</sup> granulocytes with GM-CSF or CD8<sup>+</sup> T cells with IL-15, respectively. Whereas the GM-CSF-mediated signaling cascade relied exclusively on JAK2, IL-15-dependent stimulation of T cells required both JAK1 and JAK3 activities. Both 50 and 100 mg/kg doses of R723 induced strong inhibition of STAT5 phosphorylation after GM-CSF and, to a lesser extent, IL-15 stimulation, especially when a 50 mg/kg dose of R723 was administered (Figure 1A). We consistently observed a preference for targeting the JAK2-dependent GM-CSF pathway, especially at the 50 mg/kg dose 1 hour after dosing.

#### R723 inhibits erythropoiesis in a PHZ-induced hemolytic anemia model

To investigate the ability of R723 to inhibit JAK2 *in vivo*, we used the acute mouse model based on induction of anemia on PHZ treatment.<sup>31</sup> PHZ-induced RBC damage and sequential depletion lead to hyperstimulation of normal and EMH accompanied by transient splenomegaly, followed by quick (7-10 days) recovery to normal hematocrit levels. As expected, 3 days after the first PHZ injection, both hematocrit and RBC values in all groups dropped to an average of 66% and 64% of naive controls, respectively. On days 6 and 8, however, progressive recovery was observed in vehicle control animals, whereas animals administered R723 showed a dose-dependent and significant ( $P < .05$ ) delay in recovery (Figure 1B), with the 75 mg/kg twice daily dose producing the strongest effect on both parameters ( $P < .01$ ).

#### R723 is effective in an acute Ba/F3-JAK2V617F leukemia model

We investigated the effect of R723 in a mouse leukemia model relying on the use of murine Ba/F3 cells expressing JAK2V617F as a driver of cell proliferation. This model is particularly aggressive, with a lethal outcome within 15 days of cell injection in vehicle-treated mice. In the R723-treated group, we observed a small (2 days, 13%) but highly significant improvement in survival ( $P < .004$ ) compared with the vehicle-treated cohort (supplemental Figure 4). In another study, animals were killed on day 13, before the full disease onset, to evaluate the levels of green fluorescent protein-positive (GFP<sup>+</sup>) Ba/F3-JAK2V617F cells in the spleen and BM. We observed a significant decrease in spleen cellularity and in

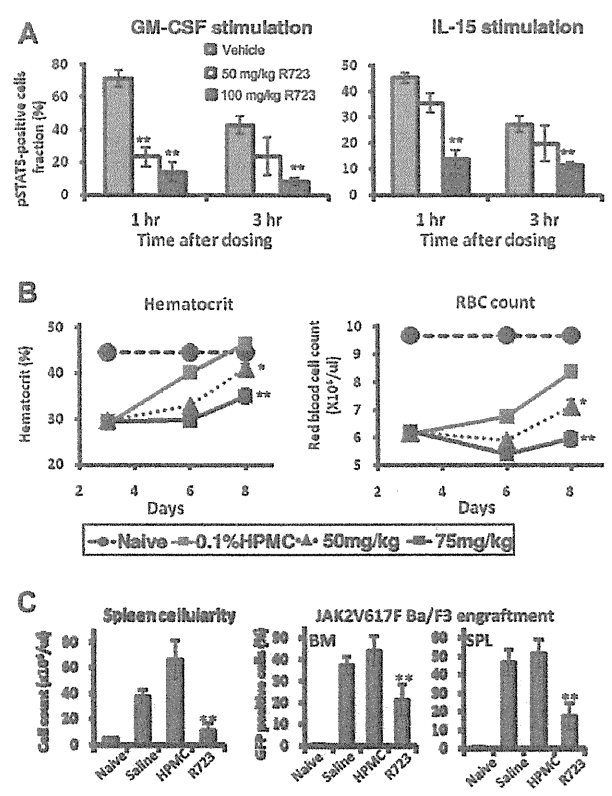


**Figure 1. R723 shows selectivity and efficacy in mice.** (A) Analysis of JAK2- and JAK1/JAK3-dependent STAT5 phosphorylation in primary cells. WT mice (female BALB/c) were orally dosed with vehicle, R723 50 mg/kg, or R723 100 mg/kg. Blood was collected at 1 and 3 hours after dosing and stimulated with either GM-CSF or IL-15. The percentage of pSTAT5-positive Gr-1<sup>+</sup> cells with GM-CSF stimulation (left panel) and the percentage of pSTAT5-positive CD8<sup>+</sup> cells with IL-15 stimulation (right panel) at each time point are shown. (B) R723 is efficacious in the hemolytic anemia mouse model. Hematocrit (left panel) and RBC count (right panel) changes were examined in mice administered PHZ on days 0 and 1 followed by oral daily administration of R723 or vehicle on days 2-7. Hematocrit and RBC counts of naive mice on day 3 were used as a baseline. (C) NOD/SCID mice injected with Ba/F3-JAK2V617F cells were administered with saline, vehicle (hydroxypropyl methylcellulose), or 50 mg/kg of R723 twice daily. Spleens and BM were harvested 13 days after cell injection. Cell counts per spleen (left panel) and percentage of GFP<sup>+</sup> cells (Ba/F3-JAK2V617F) in BM and spleen cells (right panel) are shown. Data are presented as means ± SE. \*\*P < .01; \*P < .05.

GFP<sup>+</sup> cells in BM and spleen from R723-treated mice compared with those from untreated or vehicle-treated mice (Figure 1C).

**In vitro growth inhibition of JAK2V617F-harboring hematopoietic cells by R723**

We investigated the effect of R723 in a murine model of MPN induced by JAK2V617F. H2K<sub>b</sub> promoter-controlled JAK2V617F-expressing mice (V617F-TG) show extreme leukocytosis, thrombocytosis, and progressive anemia,<sup>9</sup> as well as hepatosplenomegaly with EMH, megakaryocytosis, and fibrosis in the BM. BM cells show constitutive activation of STAT5 and formation of cytokine-independent growth of CFU-E colonies (as is also seen in JAK2V617F-positive MPN patients) and exhibit high mortality compared with WT mice. These features of V617F-TG closely resemble PMF patients and their progression.

We also investigated the in vitro efficacy of R723 on WT and V617F-TG BM cells by assessing STAT5 activation in Mac-1/Gr-1<sup>+</sup> cells. Cells were starved of growth factors for 4 hours and then stimulated with IL-3, EPO, and G-CSF. V617F-TG myeloid cells had more phosphorylated basal levels of STAT5 than WT

myeloid cells, and after IL-3 + EPO + G-CSF stimulation, the degree of phosphorylation further increased. In vitro treatment of V617F-TG myeloid cells with R723 resulted in a marked decrease in phosphorylation of STAT5 (Figure 2A). These data indicate that R723 is capable of inhibiting activation of STAT5, the main effector of JAK-STAT signaling, in primary hematopoietic cells expressing JAK2V617F.

We next assessed the effect of R723 on EPO-independent colony formation. R723 inhibited EPO-independent CFU-E growth of BM cells from V617F-TG in a dose-dependent manner. A 5-fold reduction at 800nM R723 was observed (Figure 2B). Cytokine-dependent colony formation (CFU-E, CFU-GEMM, CFU-GM, and BFU-E) was also inhibited by the presence of R723. In all colony types, R723 inhibited colony growth of both V617F-TG and WT cells at the same level (Figure 2C). This agrees reasonably well with the results of a 2-point in vitro kinase assay in which R723 showed an identical inhibition profile for both WT and the V617F mutant of JAK2 (supplemental Table 1).

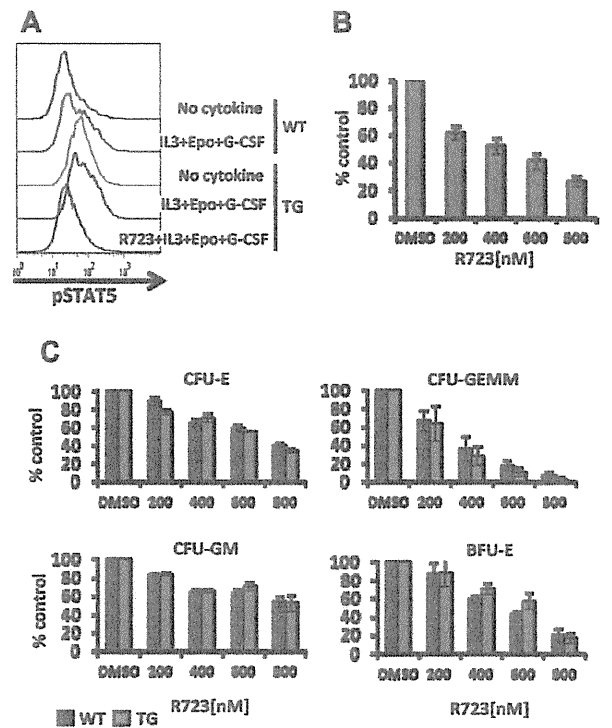


**Figure 2. R723 inhibits JAK/STAT signaling and growth of JAK2V617F harboring hematopoietic cells.** (A) BM cells from WT or V617F-TG mice were harvested and cultured without serum for 3 hours. Cells were incubated with vehicle or R723 for 1 hour, followed by the stimulation with IL-3, EPO, and G-CSF for 15 minutes. Mac-1/Gr-1<sup>+</sup> myeloid cells were analyzed for levels of STAT5 phosphorylation by flow cytometry. One representative experiment of 3 is shown. (B) Effects of R723 on EPO-independent CFU-E colonies derived from V617F-TG. BM cells from V617F-TG were cultured in duplicate in methylcellulose culture medium in the absence of EPO with and without R723. The number of CFU-E colonies was counted on day 3. R723 treatment significantly suppressed CFU-E in V617F-TG. Three independent experiments were performed. Data are presented as means ± SE. (C) Effects of R723 on cytokine-dependent BM colonies derived from WT and V617F-TG mice. BM cells from WT and V617F-TG mice were cultured in cytokine-containing methylcellulose with and without R723. The number of CFU-E colonies was counted on day 3 (top left). The numbers of CFU-GEMM (top right), CFU-GM (bottom left), and BFU-E (bottom right) colonies were counted on day 7. R723 inhibited the cytokine-dependent colonies (CFU-E, CFU-GEMM, CFU-GM, and BFU-E) derived from both WT and V617F-TG cells to the same extent. Three independent experiments were performed, each using 1 different WT mouse and 1 different V617F-TG mouse. Data are presented as means ± SE.

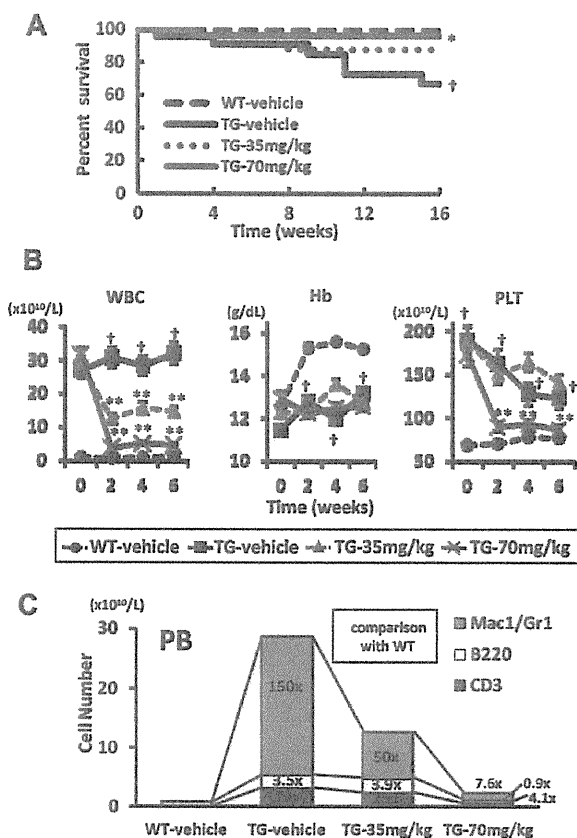


**Figure 3. Survival and changes of PB of V617F-TG mice treated with R723.** (A) Kaplan-Meier plot of WT mice treated with vehicle (WT-vehicle) and V617F-TG mice treated with vehicle (TG-vehicle), 35 mg/kg of R723 (TG-35mg/kg), or 70 mg/kg of R723 (TG-70mg/kg) for 16 weeks. There was a statistical difference in survival between the TG-vehicle group and the WT-vehicle group ( $\dagger P < .01$ ) and between the TG-70mg/kg group and the TG-vehicle group ( $* P < .05$  by log-rank test). (B) Differential blood counts in WT-vehicle and TG-vehicle, TG-35mg/kg, or TG-70mg/kg treated with R723 for 6 weeks. V617F-TG mice showed severe leukocytosis and thrombocytosis at 12 weeks of age compared with age-matched WT mice ( $\dagger P < .01$ ). The leukocyte and platelet count in V617F-TG mice treated with R723 was significantly reduced compared with the TG-vehicle group ( $** P < .01$ ). V617F-TG mice had anemia ( $\dagger P < .01$ ) that was not improved by R723 treatment. Data are presented as means  $\pm$  SE. (C) Hematopoietic compartment of PB assessed by flow cytometry. At 18 weeks of age in the TG-vehicle group, the Mac-1/Gr-1<sup>+</sup> myeloid cells were significantly increased in number and the B220<sup>+</sup> B cells and CD3<sup>+</sup> T cells were increased to a lesser extent than myeloid cells. R723 treatment for 6 weeks significantly decreased the number of Mac-1/Gr-1<sup>+</sup> myeloid cells ( $P < .01$ ) and mildly decreased the number of B220<sup>+</sup> B cells and CD3<sup>+</sup> T cells ( $P < .05$ ). Data are means of 6 mice in each group.

### R723 effectively improves survival, leukocytosis, and EMH in JAK2V617F-induced murine MPN

At 12 weeks of age, all V617F-TG mice developed MPN exhibiting leukocytosis, with average white blood cell counts of  $29 \times 10^{10}/L$ . V617F-TG mice were divided into 3 groups and treated with R723 by oral gavage at 35 mg/kg twice daily (TG-35mg/kg;  $n = 30$ ), 70 mg/kg twice daily (TG-70mg/kg;  $n = 26$ ), or vehicle twice daily (TG-vehicle;  $n = 23$ ) for 16 weeks. As a control for TG-vehicle, we prepared WT mice treated with vehicle (WT-vehicle;  $n = 30$ ). During the study, 6 of 23 in the TG-vehicle group and 3 of 30 in the TG-35mg/kg group died, whereas only 1 of 26 mice in the TG-70mg/kg group died (Figure 3A). Therefore, administration of R723 at 70 mg/kg twice daily significantly improved the survival of V617F-TG mice ( $P < .05$ ).

V617F-TG mice at 12 weeks of age had severe leukocytosis (Figure 3B). After 2 weeks of R723 treatment, the leukocyte count was reduced to 45% in the TG-35mg/kg group ( $P < .01$ ) and to 13% in the TG-70mg/kg group ( $P < .01$ ) compared with the TG-vehicle group, and the effect was maintained until the end of the study (Figure 3B). In V617F-TG mice, not only Mac-1/Gr-1 myeloid cells, but also B220<sup>+</sup> B cells and CD3<sup>+</sup> T cells increased in number. Compared with the numbers in WT, the numbers of myeloid cells, B cells, and T cells were increased by 150-fold, 3.5-fold, and 19-fold, respectively (Figure 3C). After 6 weeks of 70 mg/kg R723 treatment in V617F-TG mice, the number of PB myeloid cells, B cells, and T cells reached 7.6-fold, 0.9-fold, and 4.1-fold, respectively, compared with that in WT (Figure 3C). Although R723 treatment reduced the number of all types of PB cells in a dose-dependent manner, the reduction of myeloid cell number was the most significant ( $P < .01$ ): to less than one-tenth of that of the TG-vehicle group. A reduction in platelet count of 48% was observed in the TG-70mg/kg group ( $P < .01$ ) compared with the TG-vehicle group (Figure 3B). Because platelet numbers in the TG-vehicle group were reduced gradually in the natural disease course, the difference between the 2 groups disappeared after 9 weeks of treatment. In contrast to the effect on leukocyte and platelet numbers, there was no improvement in anemia in V617F-TG mice treated with R723 (Figure 3B).

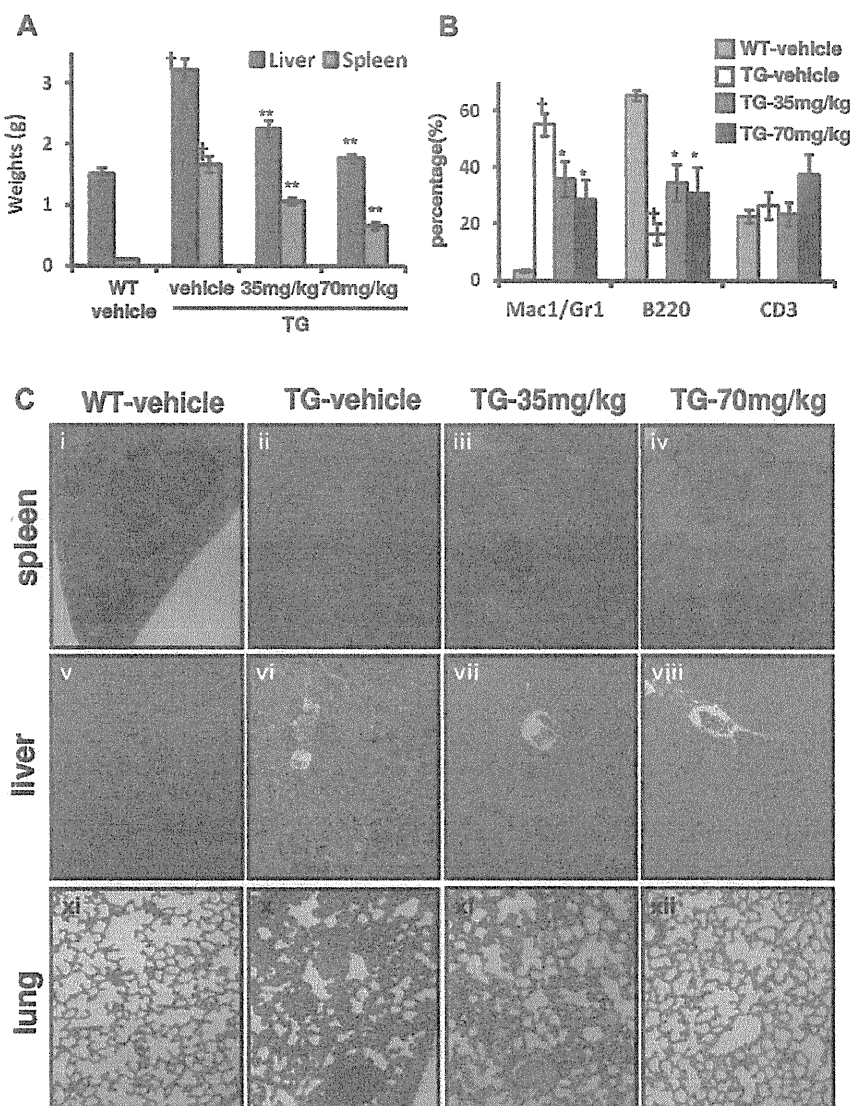
R723 treatment also improved hepatosplenomegaly in V617F-TG mice in a dose-dependent manner (Figure 4A). In the spleen, Mac-1/Gr-1<sup>+</sup> myeloid cells associated with EMH were significantly decreased, and B220<sup>+</sup> B cells were relatively increased by R723 treatment (Figure 4B). Along with reduction of organ weights and infiltrating myeloid cells, there was also clear evidence of a dose-dependent reduction in histopathology of EMH in the spleen, liver, and lungs from R723-treated V617F-TG mice (Figure 4C). Histopathological analysis of spleens from the TG-vehicle group exhibited complete effacement of normal splenic architecture and invasion of myeloid cells, whereas R723 treatment resulted in a marked reduction of cell invasion and restored architecture in V617F-TG spleens. Changes in the liver and lungs were more dramatic. FMH consisting of infiltrates of maturing myeloid cells and megakaryocytes seen in the TG-vehicle group were reduced in a dose-dependent manner by R723 treatment and almost completely disappeared in the TG-70mg/kg group (Figure 4C). In contrast to the drastic pathological improvement in spleen, liver, and lung (Figure 4C), R723 had little effect on the progression of fibrosis and megakaryocyte hyperplasia in BM (data not shown).

We also evaluated the histopathological toxicity of R723 in the brain, heart, kidney, ovary, testes, and gastrointestinal tract. There were no signs of toxicity related to R723 in any tissue examined at either the 35 mg/kg or the 70 mg/kg dose.

Transplantation of BM cells from V617F-TG causes MPN in WT recipient mice. These mice exhibited granulocytosis, splenomegaly, EMH, and mild BM fibrosis. CD45.2<sup>+</sup> BM cells from V617F-TG mice were injected into irradiated recipient WT mice, together with CD45.1<sup>+</sup> WT BM cells. Twenty weeks after BM transplantation, we administered R723 or vehicle by oral gavage at 70 mg/kg twice daily for 4 weeks. As shown in Table 3, R723 treatment decreased the number of leukocytes, especially in Mac-1<sup>+</sup> or Gr-1<sup>+</sup> myeloid cells, in recipient mice. The number of B or T lymphocytes in the PB was not affected by R723 treatment, nor was the hemoglobin value or platelet number. In recipient mice, the number of CD45.2<sup>+</sup> V617F-TG-derived cells decreased, whereas CD45.1<sup>+</sup> WT-derived cells remained unchanged by R723 treatment, indicating that R723 selectively inhibited cells harboring V617F JAK2. A 5-fold reduction in spleen weights in R723-treated

**Figure 4. Improvement of hepatosplenomegaly and EMH in V617F-TG mice treated with R723 for 6 weeks.**

(A) R723 effects on liver and spleen weights after R723 treatment for 6 weeks. Liver and spleen weights in V617F-TG mice treated with vehicle (TG-vehicle) were increased compared with those in WT mice treated with vehicle (WT-vehicle) ( $\dagger P < .01$ ). R723 treatment in V617F-TG mice significantly reduced organ weights ( $**P < .01$ ). Data are presented as means  $\pm$  SE. (B) Hematopoietic compartment of spleen assessed by FACS. The proportion of Mac-1/Gr-1<sup>+</sup> myeloid cells significantly increased, and that of B220<sup>+</sup> B cells decreased in 18-week-old TG-vehicle mice compared with age-matched WT-vehicle mice ( $\dagger P < .01$ ). R723 treatment in V617F-TG mice for 6 weeks decreased the proportion of Mac-1/Gr-1<sup>+</sup> myeloid cells and increased the proportion of B220<sup>+</sup> B cells ( $*P < .05$ ). The percentage of CD3<sup>+</sup> T cells was constant. Data are presented as means  $\pm$  SE. (C) Histological changes in V617F-TG mice by R723 treatment for 6 weeks. Histology of WT-vehicle and V617F-TG mice treated with vehicle, 35 mg/kg, and 70 mg/kg doses of R723 (TG-vehicle, TG-35mg/kg, TG-70mg/kg, respectively). Cells were stained with H&E. In the spleens of the TG-vehicle mice, the red pulp was expanded with maturing myeloid cells and megakaryocytes and the white pulp was scarce compared with WT-vehicle mice (i-ii). Mice treated with R723 for 6 weeks showed marked reduction of myeloid cell invasion and partially restored architecture (iii-iv). Liver and lung sections from TG-vehicle also displayed EMH (vi and x). Infiltration of myeloid cells disappeared with R723 treatment in V617F-TG mice (vii, viii, xi, xii).



recipient mice compared with the vehicle-treated recipient mice was also observed. R723 treatment caused a significant reduction of BM fibrosis (supplemental Figure 5), although the degree of myelofibrosis severity in recipient mice was much milder than that in V617F-TG mice.

**The effect of R723 on BM progenitor cells in V617F-TG mice**

FACS was performed on BM cells in V617F-TG mice treated with R723 or vehicle. In V617F-TG mice, the proportion of LSK and GMP cells increased ( $P < .01$ ) and the proportions of CMP, MEP,

**Table 3. In vivo effect of R723 on JAK2 V617F-harboring cells**

	Vehicle (n = 5)		R723 (n = 5)	
	Pretreatment	Posttreatment	Pretreatment	Posttreatment
White blood cells, $\times 10^9/\mu\text{L}$	19.8 (10.8-28.5)	19.8 (10.2-31.8)	15.0 (11.7-25.2)	10.8 (8.1-15.3)*
Mac-1 <sup>+</sup> or Gr-1 <sup>+</sup> myeloid, $\times 10^9/\mu\text{L}$	10.7 (3.2-19.2)	11.4 (3.7-22.3)	7.9 (6.4-20.2)	4.6 (3.1-9.2)*
B220 <sup>+</sup> B cells, $\times 10^9/\mu\text{L}$	2.1 (0.4-9.6)	2.0 (0.4-9.1)	1.9 (0.8-5.1)	2.5 (0.8-3.6)
CD4 <sup>+</sup> or CD8 <sup>+</sup> T cells, $\times 10^9/\mu\text{L}$	4.0 (3.0-7.2)	2.8 (2.7-7.5)	4.2 (3.4-4.7)	3.6 (3.1-4.6)
CD45.1 <sup>+</sup> cells, $\times 10^9/\mu\text{L}$	1.5 (0.8-12.3)	1.6 (0.7-11.2)	1.5 (0.7-8.1)	1.3 (0.7-4.4)
CD45.2 <sup>+</sup> cells, $\times 10^9/\mu\text{L}$	12.6 (2.6-27.7)	13.0 (2.2-31.1)	11.1 (6.9-24.5)	7.4 (4.3-14.4)*
Hemoglobin, g/dL	11.3 (11.2-13.9)	11.1 (10.7-14)	12.5 (11.2-14.5)	12.9 (10.7-14.3)
Platelets, $\times 10^9/\text{L}$	61.9 (50.8-81)	53.2 (14-92.5)	70.8 (52-119)	106 (57.2-137)
Spleen weight, g	n.d.	0.20 $\pm$ 0.04	n.d.	0.04 $\pm$ 0.01†

Peripheral blood data are presented as medians (range). Spleen weights are presented as means  $\pm$  SE. The paired data between pretreatment and posttreatment were analyzed with a paired 2-tailed *t* test. The comparison of spleen weights between vehicle-treated mice and R723-treated mice were analyzed with a 2-tailed *t* test. n.d. indicates no data. \* $P < .05$ . † $P < .01$ .